Model-checking tool support for quantitative risk analysis and design for safety

Peter Lindsay
Kirsten Winter
Robert Colvin

August 2010

Technical Report SSE-2010-04

Division of Systems and Software Engineering Research
School of Information Technology and Electrical Engineering
The University of Queensland
QLD, 4072, Australia

http://www.itee.uq.edu.au/~sse

Model-checking tool support for quantitative risk analysis and design for safety

Peter Lindsay* Kirsten Winter Robert Colvin

School of Information Technology and Electrical Engineering,
The University of Queensland, Queensland 4072, Australia
*Email: p.lindsay@uq.edu.au

Abstract

This paper is concerned with quantitative analysis of tolerance of sensor hardware failures by control system software. The aim is to help the system designer evaluate the effectiveness of risk reduction measures in the system design. This paper proposes an approach for using stochastic model checking to evaluate how likely a given sensor failure mode is to lead to a hazardous system failure, taking control logic and sensor-update timing failures into account. In particular we propose two complementary techniques: one for examining short-term consequences of component failures and the other for examining more subtle longer-term consequences (so-called hidden failures). The techniques overcome scaling issues and yield valuable insights into the relative merits of different design decisions. The PRISM model checker is used for stochastic analysis of Continuous Time Markov Chain (CTMC) system models. The approach is illustrated on a case study from manufacturing, involving an industrial metal Press. Although relatively simple, the Press exhibits a wide range of different behaviours, including hidden failures and subtle race conditions.

Keywords: System hazard analysis ; design for safety ; FMEA ; stochastic model checking ; quantitative risk analysis ; Continuous Time Markov Chain models.

1 Introduction

Programmable Electronic Systems are increasingly being used to control safety-critical equipment [1, 2, 3]. Such systems have stringent fault-tolerance requirements, and must be designed in such a way that component failures are anticipated and their effects adequately mitigated, so that the risk of unsafe (hazardous) system behaviours is acceptably low. It can be very difficult to predict how the system will behave in the presence of component failures due to the number of circumstances that need to be taken into account, including all of the different combinations of states of the control system, the Equipment Under Control (EUC) and the environment. *Failure Modes and Effects Analysis (FMEA)* is the name typically given to this general form of analysis [4].

The process of FMEA relies heavily on the analyst's expertise and familiarity with the system design. Quantitative FMEA (also called *criticality analysis*) is used to estimate the likelihood that a given component failure mode will lead to a given hazard. It is usually done informally using approximate models [2, 5, 6]. This paper explores in depth the use of stochastic model checking with Continuous Time Markov Chain (CTMC) models to automate such analysis. The aim is to improve system designers' and analysts' understanding of the impact of design decisions on hazard likelihood, in the trade off between software complexity and system safety.

In principal, calculations which would be extremely difficult and error-prone to do by hand can be done quickly and easily by the new generation of stochastic model checkers, such as PRISM [7, 8]. This paper describes the application of PRISM to a software control system. We show that CTMC model checking is a powerful tool which can yield valuable insights into the comparative merits of different design decisions, particularly with respect to their relative effect on hazard probabilities and mean-time-to-hazardous-failure. We show that it can be used to answer questions such as:

- What are the critical components in the design, and how reliable do they need to be in order for risk of system failure to be tolerable?
- How do architectural performance issues such as data update and CPU processor rates affect likelihood of failure due to race conditions?
- Given that faults can lie dormant for some time before the conditions arise which cause a system failure to become manifest, how can the

associated risk be quantified and estimated?

We propose two complementary techniques for performing component-failure effects analysis: one for examining short-term consequences of component failures, and the other for examining more subtle longer-term consequences (so-called *hidden* or undetected failures). We also show that analysis results can be highly sensitive to modelling decisions and so must be treated with a great deal of care.

1.1 Overview of the approach

Our method begins with modelling physical aspects of the EUC using the differential equation-based simulation tool Modelica [9], and then injecting component faults into the model to investigate the circumstances under which system behaviour diverges from normal. This step helps the analyst identify critical components (or more precisely, the component failure modes which contribute to system failures), the nature of possible hazardous system behaviour, and the circumstances under which component failures give rise to system hazards (cause-consequence analysis).

The next step is to use the insights gained in order to estimate risk associated with particular component failures (criticality analysis). For these purposes we develop CTMC models of the EUC, the control-system components and their failures, and the environment (including the human operator), and then use PRISM to evaluate the likelihood of hazardous system failures. System properties, such as reability of hazardous states, are expressed in Continuous Stochastic Logic (CSL) [10].

One of the main contributions of the paper is to develop analysis methods that scale well with system operation time. This is particularly important for systems with long mission times, of the order of months or years for example, and with very low tolerable rates for hazardous system failure, such safety monitoring and control systems [1, 2]. When the cause-consequence relationship between component failures and hazards is complex, probabilistic analysis can quickly get pushed beyond the limits of computational feasibility [11]. The paper explores these limits on a well known case study and proposes practical solutions.

The approach is illustrated on an Industrial Press case study taken from the literature [12, 13]. The example is small enough to allow a detailed treatment to be undertaken here. On the other hand, scaling is already

an issue for this example because of the system's long mission time. In this paper we focus on control system design, including the control logic and data rates used. We examine the possible consequences of sensor failures and race conditions, and show how to estimate their likelihood using PRISM. We examine the effect that changes to the design have on these figures. The approach can of course be expanded to consider other component failures, but the example is already rich enough to illustrate many of the subtle issues that arise in practice.

In fact PRISM supports two other types of stochastic models [14]: Markov Decision Processes (MDPs) and discrete-time Markov chains (DTMCs). We chose CTMC modelling for several reasons. MDPs allow for non-deterministic choice, but do not support calculation of probabilities for particular behaviours (such as system hazards), although they can be used to investigate best-case and worst-case scenarios. DTMCs model time as discrete time steps, and so would allow only a coarse view of the continuous timing behaviour that is typical of most control systems. CTMCs seemed the natural choice for our application area, and indeed for our case study the resulting models are relatively simple and elegant. Also, simple hardware components are often assumed to have constant failure rates (and sometimes human operators) and this is very natural to model in CTMCs [2]. CTMC reward structures also proved very useful, as shown below.

1.2 Structure of the paper

The paper is structured as follows: Section 2 describes related work on tool support for FMEA and criticality analysis. Section 3 describes the Press case study and the Modelica model of the physical behaviour of the Press. A simple control logic is assumed initially, based on the Press operational concept. The Modelica model is used to derive values of key parameters for the CTMC model of the Press developed later in the paper. Section 4 describes how the Modelica model was used to perform a Preliminary Hazard Analysis by injecting component faults and seeing how and when system behaviour diverged from expected behaviour. We identify four hazardous and three undesirable (but not necessarily hazardous) system failure modes, and provide a preliminary mapping from component failure modes to hazards and co-effectors.

Section 5 describes the CTMC model of the Press, its control system and its environment (in this case, operator actions), together with the sensor fail-

ure modes and a means for injecting faults directly into the system model. Section 6 describes the basis of the risk calculations, including how safety requirements can be formalised for model checking in PRISM, and how the risk of short- and longer-term consequences can be estimated. Section 7 describes the results of the risk analysis applied to the initial Press design, and illustrates the effects of different CPU processor/data rates and component failure modes on hazard likelihood. The section illustrates the sensitivity of the results to modelling assumptions and establishes a baseline against which the effects of system design changes are judged in later sections. Section 8 investigates the effect of modifying the control logic to detect errors and fail to a safe state where possible, without otherwise modifying the Press design. Section 9 investigates the effect of a second possible design change, which involves altering the position of one of the sensors in order to reduce the likelihood of a hazardous race condition. Throughout the paper we report PRISM computation times, to illustrate the scaling issues of quantitative analysis. The full Modelica model is given in Appendix A. Appendix B lists the parts of the PRISM model that are omitted in the text for provide a complete design model.

2 Related work

A number of different approaches to automating FMEA have been proposed for software-based systems, including automated simulations with fault injection [15, 16], extraction and analysis of fault propagation models such as synthesized fault trees [17, 18], and model checking with fault injection [19, 20, 21, 22, 23]. Simulation-based approaches explore a set of possible traces for the cause-consequence relationship between failure modes and hazards. Like other testing approaches, simulation-based approaches generally cannot cover all of the different sets of circumstances that might arise, even in relatively small systems. Techniques that extract fault propagation models can reduce the search space to more feasible sizes, but depend critically on the completeness and correctness of the extraction process, and the insights they yield are often indirect and hard to interpret back into the system design. Model checking approaches by contrast can provide means for exhaustively exploring the state space of a given system directly and automatically.

Most of the approaches listed above are qualitative (although the fault-tree based approaches typically support a crude form of quantitative anal-

ysis). Stochastic model checking is a relatively recent development, and is finding widespread use in quantitative system reliability evaluation [7]. A number of recent papers have extended this to FMEA and the evaluation of fault tolerance [24, 25, 26].

The stochastic model checking approach is clearly very promising, but the usual scaling problems for model checking still apply. One way of dealing with the problem, as applied in [24, 25], is to assume a target tolerable hazard rate and mission lifetime and then to use the model checker to see whether the rate is exceeded over the mission time for the given system design. Usually this results in a significantly faster computation time than trying to estimate the actual hazard likelihood. However the mission times for which this approach is feasible are still relatively short. For example, the simple airbag model in [25] takes 12 hours to check hazard tolerability over a 10 hr mission time. By contrast in this paper we are concerned with mission times of over a year.

When a tolerability level is exceeded [25] proposes a way of generating a set of paths (analogous to counterexamples in standard model checking) that lead to the hazard and together exceed the tolerable probability. With the aid of a visualiser, the analyst can investigate which paths are more likely to occur, and thereby gain insights into which component failures and fault propagation mechanisms contribute most to risk.

Elmqvist *et al* [26] set probabilistic model checking in the context of more general safety assessment processes. Their approach is very similar to ours, but their example (fault tolerance in an aircraft altimeter) is a synchronous system with very simple timing behaviour and so does not address many of the issues that are important for a wide range of systems. Domínguez-Garca *et al* [27] demonstrate the use of Markov models and MatLab to support the design analyst in the evaluation of fault tolerance for a flight control system in a control theory setting (i.e., sets of differential or difference equations) but use hand-crafted tools.

Bozzano *et al* [28] propose a model-based approach to system-software co-engineering. The framework is supported by a tool chain which also includes analysis tools for quantitative and qualitative analysis to produce Fault Trees as well as FMEA tables. The report, however, does not reveal details of how the initial model is transformed into a Markov Chain model which is then put into the Markov Reward Model Checker (MRMC) [29] to check probabilistic properties. An industrial evaluation of the framework is proposed as future work.

Tool supported analysis of stuck-at faults in reconfigurable memory arrays

using the HOL theorem prover is proposed in [30]. The aim is to prove a more general relation between key statistical features of the device and its parameters, namely the number of spare rows and columns in the memory array that allows for repair solutions. This work is similar to ours in that it aims at a quantitative analysis of system behaviour in the presence of faults. However, the approach is not algorithmic and relies heavily on user expertise in driving the proof engine.

Our work is focused on developing a CTMC model and analysing it with the PRISM model checker. Other tools could have been also chosen for this task, such as the Markov Reward Model Checker (MRMC) [31] and the Erlangen Twente Markov Model Checker (ETMCC) [32] which provide similar numerical analysis capabilities for CTMCs as PRISM, but with less developed user interfaces. Vesta [33] and YMER [34] provide statistical model checking capabilities, based on Monte Carlo simulation or discrete event sampling, respectively, and statistical hypothesis testing. An experimental performance comparison between these tools can be found in [35] and a comparison between numerical versus statistical model checking can be found in [36]. Probabilistic model checking has also been integrated into various tool chains supporting formalisms such as stochastic Petri Nets [37] and Statecharts [38].

3 The case study: the Industrial Metal Press

This section describes the hypothetical case study on which the approach is illustrated, and the physical simulation that was used to derive key values for the CTMC models developed later in the paper.

3.1 Press operation and design

The Industrial Press is a hydro-mechanical system of the kind used to produce body parts for motor vehicles [13]. The main physical component of the Press is a 50 tonne plunger which gets raised 7 metres and then, upon a command from the operator, falls under gravity onto a metal workpiece, pressing it into the desired shape. The Press system includes an automated control component implemented via a Programmable Logic Controller (PLC).

The primary parts of the Press are shown in Figure 1. The plunger is raised to the top and held there by a motor drive, winding gear and hydraulic

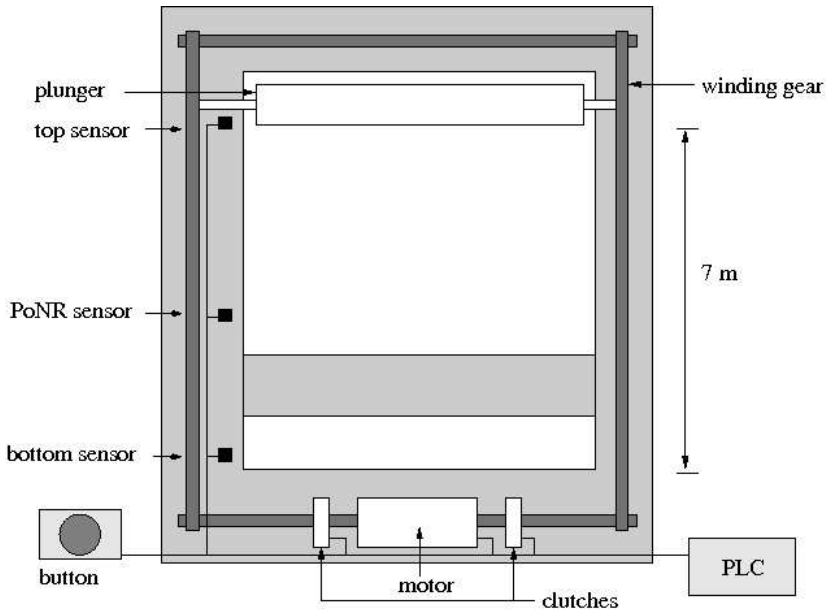

Figure 1: Press design

clutches. The Press control component activates and deactivates the motor drive in response to sensors which detect the position of the plunger and the state of the operator button. When the plunger is at the top and the operator pushes and holds down the button, the controller deactivates the motor drive and allows the plunger to fall. When the plunger reaches the bottom, the controller automatically re-activates the motor drive and the Press re-opens.

The control logic includes as a safety feature the ability for the operator to abort operation by releasing the button while the Press is closing. This causes the controller to reactivate the motor drive and re-open the Press. Note however that there is a point – called the *Point of No Return (PONR)* – after which the falling plunger's momentum is so high that it is not feasible to prevent the Press closing. Activating the motor drive after this point will only slow the plunger's descent but not stop it closing, and may even damage or destroy the opening mechanism. The control system thus also includes a PONR sensor and only permits closing to be aborted if the plunger has not yet reached the PONR.

Under normal operation the Press will close in approximately 2 seconds, and open in approximately 4 seconds. The Press would typically be operated

Abbreviation	Meaning	Value
Given values:		
H	Height	7.0 m
TTO	Time to open	4.0 s
TTC	Time to close	2.0 s
Calculated values:		
PONR	Height of PONR	1.44 m
TTP	Time to fall to PONR under gravity	1.780 s
RTP	Time to rise from bottom to PONR	1.883 s
TTR	Time to reopen fully after abort (worst case)	4.5 s

Table 1: Press distance and time values

once per minute (i.e., a full operational cycle would typically take 60 sec). There would normally be 420 operations of the Press per day and approximately 10^5 per year. It is estimated that operation would be aborted roughly once in every 100 press operations.

In this paper we are primarily concerned with the Press control system software design, including the control logic and data rates used. We examine the different possible consequences of sensor failures and race conditions, and show how to estimate their likelihood using PRISM. We examine the effect of design changes on these figures. The approach can of course be expanded to consider other component failures, such as the motor drive and winding gear or the PLC itself, but the example is already rich enough to illustrate many of the subtle issues that arise in practice.

3.2 Modelling Press behaviour and component failures

In order to derive values for the key parameters of our CTMC models, we first developed a physical simulation of the system in Modelica [9], using the laws of physics for constant motor-drive force with friction. A value for the motor-drive force was estimated and the value of the friction coefficient was adjusted until a close match was achieved with the Press opening and closing times given above. A very simple control logic was derived to match the operational concept above: the motor gets turned off if the plunger is at the top and the button gets pushed; the motor gets turned on again when the plunger reaches the bottom or if the button is released while the

plunger is above the PONR (the abort case). The values for the other key parameters, such as the height of the PONR, were then calculated from the model: Table 1 presents the results. (The TTR case corresponds to activating the motor drive immediately before PONR, so that the press almost, but not quite, closes fully.) The full model is given in Appendix A.

The Modelica model was built in such a way that component failures can be injected to help the analyst identify the kinds of system failure that might eventuate. Section 4 below describes the Preliminary Hazard Analysis process and the support Modelica provides. The most common forms of control system input failures, and the ones whose effects last the longest, are persistent ("stuck at") failures, whereby a sensor component "breaks" and the control system receives a constant value from that time onwards [2]. There could be many different causes of this: the sensor itself could break or lose its connection with the plunger, the communication link between the sensor and the control component could break, the PLC input register or the read mechanism could fail, and so on. In the case of the Press control system, there are four different sensors and hence eight different component failure modes.

4 Preliminary Hazard Analysis

This section describes how the physical model of the Press in Modelica can be used to establish cause-consequence relationships between component failures and *system hazards* (system failure modes that could lead to accidents). In some cases there is a delay between when the component fails and when the system fails. In other cases the system failure occurs only when particular sets of conditions (called *co-effectors*) occur, such as particular operator actions being taken in particular phases of Press operation. By injecting component failures into the Modelica model, we can investigate when and how system behaviour diverges, thereby getting insight into the failure mechanisms and co-effectors involved. More specifically, we are able to formulate the different kinds of system behaviour that will be investigated more thoroughly using model checking.

4.1 Method

The effects of component failures can be investigated by running two Modelica models in parallel in the same environment: one for normal behaviour as described in the operational concept above, and one for behaviour in the presence of a failed component. A system failure occurs when the two behaviours diverge (that is, the system with a failed component behaves differently from normal). For safe operation it is necessary to consider cases when the operator pushes and/or releases the button at various different times in the operational cycle, not just at "normal times". These are the coeffectors for the Press case study. For example, although the operator would not normally push the button while the Press is opening, there is still the possibility that they may do so, and the Press should continue to behave as expected (in this case, continue to open).

A series of experiments was set up, in which one of the 8 sensor failure modes was injected 1 sec into the first operational cycle and one of 4 co-effectors took place in the second operational cycle (see below). The plunger's height was plotted as a function of time in each case where divergence occurred, and the resulting system failure modes were categorised according to the nature of the divergence. The four different environmental conditions (co-effectors) were as follows:

- operator releases the button 1 sec after pushing it – corresponding to the abort case (since from Table 1 it takes the plunger 1.78 sec to fall to PONR)
- operator releases the button 1.8 sec after pushing it – corresponding to releasing the button after PONR but before the Press has fully closed
- operator releases the button 3 sec after pushing it – corresponding to releasing the button after the Press has fully closed
- operator pushes the button while the Press is opening

In a more systematic exploration of the consequences of component failures we would also vary the time (or at least, operational phase) at which the component failed. In the results reported in the next section we considered only the case where the sensor failed as the Press was opening. This turns out to be sufficient to reveal a wide range of divergent behaviours, enough to formulate hazardous behaviours to be investigated using model checking below.

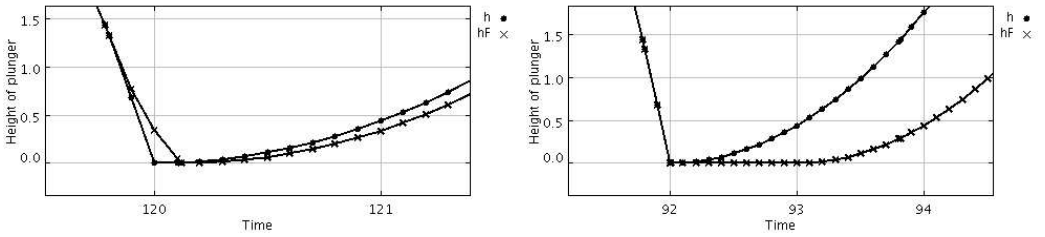

Figure 2: Normal Press behaviour (h) vs behaviour after PONR sensor fails stuck low (hf): (a) button released before Press closes; (b) button released after Press closes

4.2 Results

This section summarises the results of the experiments and identifies the system failure modes that were revealed.

4.2.1 Button sensor failure

For the simple control system design considered here, the most clearly hazardous Press failure occurs if the button sensor fails stuck high (indicating that the button is pushed). The Press will start to close again unexpectedly and uncontrollably as soon as the plunger reaches the top. We formulate the corresponding system failure as 'H1: Uncommanded closing'. No co-effectors are needed in this case: the faulty behaviour is independent of the operator's actions. This is an example of a failure where there is a delay between the cause (the button sensor fails) and the consequence (the system fails).

There is another, more subtle case involving the button sensor fails stuck high case: if the failure occurs while the Press is closing but before the operator attempts to abort by releasing the button above PONR, then abort will fail. This case would not be revealed by our simple testing strategy above. The model checking in Section 7.2.1 below does however reveal it.

If the button sensor fails stuck low then the Press will simply fail to close again. For the purposes of hazard analysis below, we treat this as an undesirable, but not hazardous, system failure 'F1: Stuck open'.

4.2.2 PONR sensor failure

Our experiments revealed two different kinds of system failure involving the PONR sensor fails stuck low case (indicating that the plunger is above the PONR). The first occurs when the operator releases the button between PONR and bottom: in normal operation the plunger should continue to fall under gravity to the bottom, but its fall is slowed in this case. Closer inspection, shown on the bottom of Fig. 2a, reveals that the plunger decelerates during the last part of its fall, suggesting that the motor drive has activated after PONR. This is a hazardous behaviour because, for reasons given in section 3.1 above, the motor drive must not activate after the PONR is passed. We categorise this as hazard 'H2: Dangerous motor activation'.

The second case occurs when the operator releases the button after the Press has closed (Fig. 2b). Rather than immediately rising after hitting the bottom as expected, there is a one second delay before the plunger begins rising. While this is not hazardous behaviour, it is clearly undesirable, and is categorised as 'F3: Incorrect opening'.

If the PONR sensor fails stuck high there is a hazardous failure in the case where the operator attempts to abort: the plunger continues to fall to the bottom. We categorise this as hazard 'H4: Abort fails'.

4.2.3 Top sensor failure

Our experiments revealed two different kinds of system failure in the top sensor fails stuck high case (indicating that the plunger has reached the top). The first occurs in the case where the operator does not release the button until after the Press has closed: this results in a delay in re-opening of the Press similar to above (F3), since the motor only comes on (and stays on) once the button is released. The other case is when the operator pushes the button while the Press is opening, which results in the motor being deactivated unexpectedly. We categorise this as hazard 'H3: Unexpected closing'. If the top sensor fails stuck low, the Press will not close again after the plunger has reached the top (system failure F1 above).

4.2.4 Bottom sensor failure

Finally, if the bottom sensor fails stuck high (indicating that the plunger has reached the bottom), we get behaviour F1 (stuck open). If the bottom sensor

ID	System failure	Description
Hazardous:		
H1	Uncommanded closing	Press starts to close without operator pushing button
H2	Dangerous motor activation	Motor activated while Press closing below PONR
H3	Unexpected closing	Motor deactivated while Press opening
H4	Abort fails	Operator unsuccessfully tries to abort Press closing
Non-hazardous:		
F1	Stuck open	Press won't close
F2	Stuck closed	Press won't open
F3	Incorrect opening	Press doesn't open until operator releases button

Table 2: System failure modes

fails stuck low, the Press does not open again. We categorise this as system failure 'F2: Stuck closed'.

4.3 Discussion

The system failure modes are summarised in Table 2. In cases where the system failure did not manifest itself under all environmental conditions, the required co-effector was also noted: see Table 3. The results of the analysis, and in particular the insights gained from detailed observation of the system, are used to inform the quantitative analysis as explained in following sections.

A larger experiment, in which the phase in which the sensor failure is also varied, would reveal further cases for Table 3. For example, H2 (dangerous motor activation) would occur if the bottom sensor failed high during the final phase of closing. Similarly, H4 (loss of abort) would occur if the button sensor failed stuck high during the initial phase of closing and the operator tried to abort.

Although the experiments reported above did not exercise all possible conditions, the system failure modes have been defined in a general way so that it is clear by inspection that they cover all the main system hazards. (See section 5.3 for formal definitions.) Adequate identification and characterisa-

Sensor	Failure mode	Co-effector	System failure
Button	stuck high		H1
	stuck low		F1
Bottom	stuck high		F1
	stuck low		F2
Top	stuck high	Button pushed while opening	H3
		Button released after Press closes	F3
	stuck low		F1
PONR	stuck high	Button released between top & PONR	H4
	stuck low	Button released between PONR & bottom	H2
		Button released after Press closes	F3

Table 3: Partial Failure Modes and Effects Analysis

tion of hazards is an important pre-requisite for subsequent risk analysis, but is beyond the scope of the current paper.

As a final remark, it should be noted that the operational concept for the Press from Section 3.1 can be implemented in several different ways, and that the choice has a large effect on the risk analysis results. As explained in Section 3.2, the "naive" control logic used in this paper is the following:

- if the plunger is at the bottom, or is above PONR and the button is released, turn the motor on
- if the plunger is at the top and the button is pushed, turn the motor off

By contrast, Atchison *et al* [13, 16] use a control logic based on (an internal representation of) the state of the Press along the following lines:

- if the Press is closed, or is closing above PONR and the button is released, turn the motor on
- if the Press is open and the button is pressed, turn the motor off

While the two logics are indistinguishable when sensors are functioning correctly, they have very different behaviours in the presence of faults. For example, if the PONR sensor fails stuck low (indicating the plunger is above the PONR), then the Press will stay in the "closing above PONR" state in

the latter case, and the motor will not get turned on again until the operator releases the button. In our case however the motor gets turned on again as soon as the plunger reaches the bottom.

Grunkse et al [24] use the same control logic as us but a different model of operator behaviour, in which the operator pushes and releases the button at a rate of once per 10 sec on average. This leads to quite different risk analysis results for some failure modes, such as PONR stuck high. They also assume that sensor values are updated and processed without delay, which is different from our treatment below (see Section 6.5.1 for details).

5 Stochastic model of the Press system

Having performed Hazard Identification and a form of Failure Modes and Effects Analysis, the next step is to develop stochastic models of the system, in order to quantify the different possible effects of component failures and estimate the likelihood of hazardous system failure. This section begins with a description of formulation of CTMCs in PRISM as background to our models. It then outlines the PRISM model of the Press. Section 5.3 outlines timing considerations and Section 5.7 describes how sensor failures are modelled. The PRISM simulator was used to manually validate timing and probability of individual transitions in the models reported below, to ensure they approximated the behaviours of the plunger and operator described in Section 3.

5.1 Stochastic modelling in PRISM

CTMCs are specified as collections of interacting modules in PRISM, each with its own variable set, initial state and set of labelled transitions [14]. Each transition is of the form

```
[e] guard -> r: var'=b
```

where `e` is an event label (used for synchronisation of transitions across different modules; the event label is omitted if the transition is not required to synchronise with transitions in other modules), `guard` is a Boolean expressions representing the guard of the transition, `r` is a rate (explained below), and `b` is the value of the variable `var` after the transition has taken place. The state of a module is determined by the current values of its variables.

The system state is the product of the individual module states. See [8] for a fuller description of the PRISM semantics.

In CTMCs, stochasticity is modelled using exponential functions for probability and timing of transitions between pre- and post-states. The modeller specifies a *rate* for each state transition. If in some state s a single transition is enabled with rate r, then the probability that the system leaves that state before time t is given by the Cumulative Distribution Function (CDF)

$$Exp_x(t) = 1 - e^{-t/x} \tag{1}$$

where $x = 1/r$. (The case where multiple transitions are enabled simultaneously is discussed below.) This treatment has some very nice mathematical properties. For example, the expected time that the system will stay in the pre-state s is x. (The actual transition to a post-state is taken to be instantaneous.) If in particular the transition goes from a working state to a failed state, then r is called a failure rate and x gives the Mean Time To Failure (MTTF).

For many aspects of our models below, 'expected time in a state' is a more natural concept than 'rate' so we tend to use x in preference to r when explaining the models below. Thus, we talk about sensors having a MTTF of 5 years, for example, when the transition leading to the failure state has a constant failure rate of 1 in 5 years. We model different phases of the Press operational cycle as discrete states, with the expected time spent in each state defined according to the values given by the Modelica simulation of plunger behaviour in Table 1 above. Thus for example, the transition from state 'plunger falling above PONR' to state 'plunger falling below PONR' has a rate of 1/TTP, which results in an expected time of TTP = 1.78 sec for being in the state 'plunger falling above PONR'.

Where transitions in two or more separate modules are synchronised (via the event label), they take place simultaneously as a single system state transition. The rate of the combined transition is the product of the rates of the individual transitions. Synchronised transitions can only be taken if the guards of all their individual transitions hold.

5.2 Race conditions

According to PRISM's semantics of CTMCs, when two or more (non-synchronised) transitions are enabled simultaneously, one of the transitions is selected prob-

abilistically and then taken: i.e., there is a "race" between the different transitions, with only one winner. Using the notation of [14], let S be the set of all states in the full CTMC model and let $R : S \times S \to \mathbb{R}_{\geq 0}$ be its transition rate matrix. The time spent in state s before any transition occurs is probabilistic with cumulative probability given by the CDF in formula 1 above, with rate r substituted by

$$E(s) \stackrel{def}{=} \Sigma_{s' \in S} R(s, s')$$

$E(s)$ is called the *exit rate* for state s. The probability of making transition $s \mapsto s'$ is given by

$$p(s, s') \stackrel{def}{=} R(s, s')/E(s).$$

and the expected time spent in the pre-state s is $1/E(s)$.

Note that this means that the timing behaviours of modules are not independent: the time that a module spends in one of its states can be influenced by behaviours of other modules. This lack of "true modularity" means the modeller needs to be very careful when specifying rates. We encountered this issue many times during modelling: cf. for example the discussion of modelling of operator behaviour in Section 5.4, estimation of Immediate Failure Likelihood in Section 6.2, and the possibility of hazardous behaviour due to race conditions in Section 6.5.1.

In the following we outline our CTMC model of the Press. This model is divided into modules corresponding to the main components of the system: the plunger, the operator, the four sensors, the control logic, and the motor-drive actuator.

5.3 Plunger behaviour

The plunger has six main physical states, according to its position and direction of travel (see Fig. 3): at bottom (state 1), rising below PONR (state 3), rising above PONR (state 4), at top (state 5), falling above PONR (state 7), and falling below PONR (state 8). Intermediate states 2, 6 and 9 are included in order to allow synchronisation of the actions of the different system components. (PRISM allows only one synchronisation event per transition.) So for example state 6 corresponds to the case where the motor has been turned off while the plunger is at the top but the plunger has not yet fallen quite far enough for the top sensor to detect its changed state. States 10-13 represent hazards H1-H4 respectively and are explained further below.

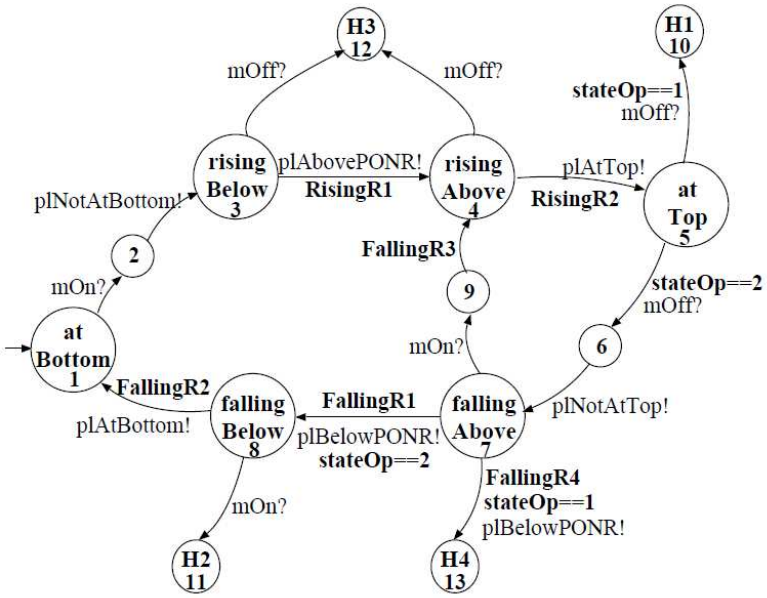


```
module Plunger
     state : [1..13] init 1;
     [motorOn]       state=1 -> state'=2;
     [plNotAtBottom] state=2 -> state'=3;
     [plAbovePONR]   state=3 -> RisingR1:(state'=4);
     [motorOff]      state=3 -> state'=12;     // H3
     [plAtTop]       state=4 -> RisingR2:(state'=5);
     [motorOff]      state=4 -> state'=12;     // H3
     [motorOff]      state=5 & stateOp=1 -> state'=10; // H1
     [motorOff]      state=5 & stateOp=2 -> state'=6;
     [plNotAtTop]    state=6 -> state'=7;
     [plBelowPONR]   state=7 & stateOp=1 -> FallingR4:(state'=13); // H4
     [plBelowPONR]   state=7 & stateOp=2 -> FallingR1:(state'=8);
     [motorOn]       state=7 -> state'=9;      // abort above PONR
     [plAtBottom]    state=8 -> FallingR2:(state'=1);
     [motorOn]       state=8 -> state'=11;     // H2
     []              state=9 -> FallingR3:(state'=4);
endmodule
```

Figure 3: Plunger behaviour

ID	System failure	Description	Plunger state
H1	Uncommanded closing	Motor deactivated while plunger at top and button released	10
H2	Dangerous motor activation	Motor activated while plunger falling below PONR	11
H3	Unexpected closing	Motor deactivated while plunger rising	12
H4	Abort fails	Plunger falls past PONR without motor being activated, even though button was released	13

Table 4: Modelling of hazardous states

Most of the transitions in our plunger model are guarded by synchronisation events. These are depicted as labels on the transition edges in Fig. 3, using the convention of adding suffix '!' or '?' according to whether the event is initiated by this component or by another component. (This notation is not part of the PRISM language and is used here only to aid understanding.) For example, the plunger transitions from rising below PONR (state 3) to rising above PONR (state 4) will synchronise with a change of state in the PONR sensor module using the event *plAbovePONR*.

Some transitions from states 5 and 7 are also guarded by a predicate whose value depends on the current state of the operator module: `stateOp=1` indicates that the operator has released the button and `stateOp=2` indicates that the operator is currently pushing the button (see Section 5.4 below). These guards are used to distinguish normal operation from hazardous behaviour. For example, if the motor gets turned off while the Press is open (state 5) and the operator is pushing the button, this is normal behaviour. But if the operator is not pushing the button, this is hazardous behaviour (H1 Uncommanded closing).

The states 10-13 model the occurrence of hazards H1-H4: see Table 4. These states are terminal states with no outgoing edges, and thus they abstract from any further behaviour of the Press that might occur after the hazardous state occurs. Modelling the hazards in this way adds some complexity to the model but it makes formalisation in CSL very easy: we simply check the likelihood that the system reaches one of the hazardous states (see

Section 6 below).

An abort by the operator is modelled as a transition from state 7 (falling above PONR) to state 4 (rising above PONR) via an additional state 9 in case the event mOn? is received. This is a slight simplification since the actual plunger behaviour will depend on how early during closing the operator releases the button. If button release occurs late (but still before PONR) then the motor will slow and eventually reverse the plunger's fall, but the plunger may pass the PONR in the interim. Rather than complicating our model by introducing complex timing considerations and force/friction calculations, we simply ignore this phenomenon, since it does not impact our main risk calculations. This simplification is valid provided we don't try to infer anything about the plunger's actual position during that phase of Press operation.

Similarly, we omitted the cases where a mOn? event is received in state 6, or a mOff? event in state 2, in the interests of simplicity. They introduced loops into the model which significantly complicated the analysis, without substantively changing the results for the hazards we study.

Timing of the plunger's behaviour

As explained above, in CTMCs all transitions are probabilistic and the system stays in a state for a non-zero period of time before transitioning to a new state. The exponential CDF describes the timing, which is parametrised by rates (see equation 1). This section explains the choice of rates in the plunger module.

The first step is to choose an appropriate unit of time for 'simple' (basic) transitions. In our model we chose to use the time taken to sense and transmit or process data, which is commonly called the *clock rate*. The actual choice of clock rate is a parameter in our model, so that we can test the effects of different design decisions. Faster clock rates reduce the likelihood of race conditions, but can be harder or more expensive to achieve in practice, so being able to evaluate the risk associated with different rates is an important capability for trade-off analysis in system design. In Section 7.1.1 below we investigate a range of clock rates from 1,000 per sec to as high a rate as our PRISM model would feasibly allow. For much of the analysis in the rest of the paper we settle on 10,000 per sec ($\texttt{clock}=10^{-4}$). Where a rate is not explicitly specified in a transition, it is taken to be the unit rate (i.e., the clock rate).

ID	Plunger state	Expected time x	x (sec)
RisingR1	3	RTP	1.883
RisingR2	4	TTO − RTP	2.117
FallingR1	7	TTP	1.780
FallingR2	8	TTC − TTP	0.220
FallingR3	9	TTP+TTR−(TTO−RTP)	4.163
FallingR4	–	TTP/2	0.890

Table 5: Derivation of rates for plunger transitions

The rates for transitions corresponding to changes in the physical state of the plunger were chosen so that the expected time spent in a state corresponds to the figures given by the Modelica simulation (see Table 1 on page 9). For example the plunger typically takes RTP=1.883 sec to rise from the bottom to the PONR with the motor on. The corresponding rate for the transition from state 3 to state 4 is thus RisingR1 = clock/RTP. The rates for the other changes of physical state of the plunger were defined similarly using Table 5. The rate FallingR3 was derived from how long it takes the plunger to start rising above PONR again if closing is aborted: we use the worst case scenario from Table 5. The rate FallingR4 was derived based on the assumption that, if the operator aborts, then the expected time for the action is halfway through the window of opportunity: i.e., TTP/2.

5.4 Operator behaviour

The operator has two possible states, *push* and *release*, according to whether they are pushing (and holding down) the button or not (see Fig. 4). The rates associated with operator behaviour are defined in Table 6. The push-button rate (PushRate) was derived from the expected time the Press spends in the open state (namely, 60 sec expected cycle time, less the 6 sec it takes to close and reopen), since pushing the button is what causes the Press to start closing during normal operation.

PushRate = clock/TAT, where TAT = 60 − (TTC + TTO)
ReleaseRateN = FallingR2
ReleaseRateA = 0.01 * FallingR1

Table 6: Rates for the operator transitions

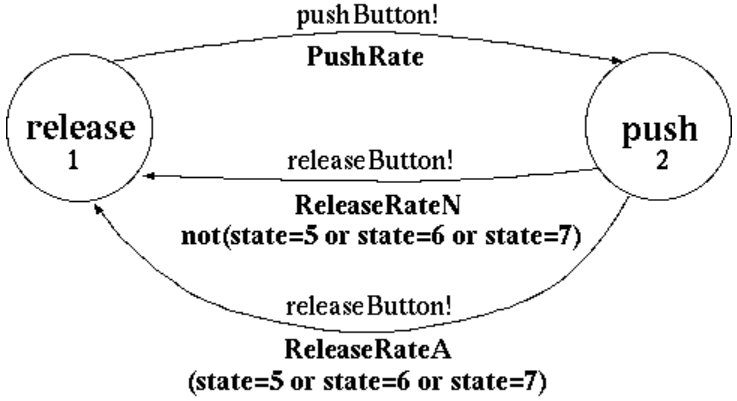


```
 module Operator
  stateOp : [1..2] init 1; // release(1), push(2)
  [pushButton]    stateOp=1
           -> PushRate:(stateOp'=2);
  [releaseButton] stateOp=2 & !(state=5 | state=6 | state=7)
           -> ReleaseRateN:(stateOp'=1); // normal release
  [releaseButton] stateOp=2 & (state=5 | state=6 | state=7)
           -> ReleaseRateA:(stateOp'=1); //  abort
endmodule
```

Figure 4: Operator behaviour

There are two different cases for when (and why) the operator releases the button. If they release the button while the Press is closing above PONR, this is an abort and we are told it typically occurs one in a hundred times. We model this by a transition which is only enabled when the plunger is in states 5-7 and whose rate (ReleaseRateA) is 0.01 times that associated with the plunger falling to the PONR (FallingR1). Thus, once the controller actions are taken, there is a race between the plunger reaching PONR and the operator releasing the button, which the PONR-reached-first case (i.e., no abort operation) is 100 times more likely to win.

The other case is where the operator releases the button normally (i.e., not while the Press is open or closing above PONR). In the absence of other information, for the purposes of analysis we have assumed the operator is equally likely to release the button before or after the Press has fully closed. By setting the rate ReleaseRateN to be the same as the rate for the plunger

transition from falling-below-PONR to at-bottom, this makes the likelihood that they release the button before the plunger reaches the bottom fifty per cent, as desired. (There is a small effect on the expected time spent in state 8 in the case where the operator keeps pushing the button because of the way exit rates are defined in PRISM, but it is negligible for the purposes of our analysis.)

5.5 Sensor and actuator normal behaviour

Sensors are modelled as simple components that detect a change in the state of the environment (such as the plunger passing a given position, or the operator pushing or releasing the button) and output a signal to the controller. Actuators detect signals and cause changes to the environment, e.g., turning the motor drive on or off.

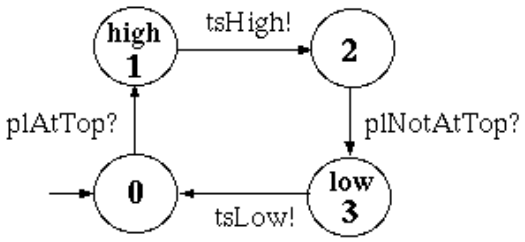


```
module TopSensor
    stateTS : [0..3] init 0;  / high(1), low(3)
    [plAtTop]    stateTS=0 -> stateTS'=1;
    [tsHigh]     stateTS=1 -> stateTS'=2;
    [plNotAtTop] stateTS=2 -> stateTS'=3;
    [tsLow]      stateTS=3 -> stateTS'=0;
endmodule
```

Figure 5: Top sensor behaviour

Fig. 5 shows the module of the top sensor. Initially the top sensor module is in state 0 and can receive event `plAtTop?` from the plunger, indicating it has reached the top. When this event occurs the module transitions to state 1 and sends the event `tsHigh!` to the controller. The sensor remains in this state until it receives event `plNotAtTop?` indicating the plunger has started

```
module Controller
   stateC : [1..2] init 1; // motor off(1), motor on(2)
   ts : [0..1] init 0;
   bs : [0..1] init 1;
   ps : [0..1] init 1;
   button : [0..1] init 0; // released(0), pushed(1)
   [buttonP]  true -> button'=1;
   [buttonR]  true -> button'=0;
   [psHigh] true -> ps'=1;
   [psLow] true -> ps'=0;
   [bsHigh] true -> bs'=1;
   [bsLow] true -> bs'=0;
   [tsHigh] true -> ts'=1;
   [tsLow] true -> ts'=0;
   [turnMOn]  stateC=1 & (bs=1 | (button=0 & ps=0))  -> stateC'=2;
   [turnMOff] stateC=2 & ts=1 & button=1  -> stateC'=1;
endmodule
```

Figure 6: PRISM code of the controller behaviour

to fall. In response the top sensor sends the event `tsLow!` to the controller and transitions to state 0 again. All these transitions have unit rate. The modules for the other sensors and the motor drive actuator are analogous to the above. They synchronise alternately with the plunger and the controller, reacting to one and causing a change in the other as a result (at least, when they are functioning correctly). The PRISM code for the other sensors and the motor component are listed in Appendix B.

5.6 Controller behaviour

The controller component keeps track of the signals it has received from the sensors and the state of the motor drive, and sends a signal to the motor drive as described in Section 3.2 above (see Fig. 6). The controller stores the current state of the sensors internally using local variables `ts`, `bs`, `ps`, `button`. Their values are updated each time a signal is received from the sensor components via the corresponding synchronisation event.

```
module TopSensor
  stateTS : [0..6] init 0;
  [plAtTop]     stateTS=0 -> stateTS'=1;
  [tsHigh]      stateTS=1 -> stateTS'=2;
  [plNotAtTop]  stateTS=2 -> stateTS'=3;
  [tsLow]       stateTS=3 -> stateTS'=0; // as before up to here
  [tsFailsHigh] !(stateTS=4 | stateTS=5 | stateTS=6)
                          -> sensorFail: stateTS'=4;
  [tsHigh]      stateTS=4 -> stateTS'=6;
  [tsFailsLow]  !(stateTS=4 | stateTS=5 | stateTS=6)
                          -> sensorFail: stateTS'=5;
  [tsLow]       stateTS=5 -> stateTS'=6;
  [plAtTop]     stateTS=6 -> stateTS'=6;
  [plNotAtTop]  stateTS=6 -> stateTS'=6;
endmodule
```

Figure 7: Top sensor behaviour with both failure modes included

5.7 Modelling sensor failures

We illustrate how to model sensor failures on the top sensor case in Fig. 7. For the purposes of the study we assume all sensors fail at a constant rate `sensorFail` (such as 1 in 5 years). We use this failure rate as a parameter of our model so that we can examine the effects of different failure rates. The sensor can either fail stuck high (e.g., the `tsFailsHigh` transition in the top sensor module) or fail stuck low (e.g., the `tsFailsLow` transition). At this point it sends one more signal to the controller (transitioning from states `4` to `6`, or `5` to `6`, respectively) and thereafter remains stuck in state 6. (The looping on state 6 is needed to allow the plunger to change states freely after the sensor has failed.) After the failure the controller receives no further signals to cause it to change its internal flag for the sensor state. Note that this way of modelling sensor failures makes no particular assumptions about the system's communications protocols, such as whether the sensor writes to registers in the controller hardware or the controller polls the sensor for values.

By contrast with all the other synchronisation events used in our model, `tsFailsHigh` and `tsFailsLow` are not actually used in any other part of the model and therefore these transitions are not synchronised. The event labels

were introduced to help in debugging and validating the model using the PRISM simulator and model checker.

When we do FMEA below only one sensor failure mode will be enabled at a time. Thus for example, when we investigate the risk associated with bottom sensor failing stuck high, we use the modules for the normal (fault-free) behaviour of the other sensors (such as Fig. 5 for the top sensor) and a copy of the module for faulty behaviour for the bottom sensor with the `bsFailsLow` failure transition removed. Similarly, when we do analysis of multiple failure modes, we include only the relevant failure transitions.

6 Risk Analysis

This section describes the basis on which the risk calculations are performed, including how various system properties can be formalised for model checking in Continuous Stochastic Logic (CSL) [10], the formal language in which properties of CTMCs are formulated for model checking in PRISM.

6.1 Hazard probabilities

Ideally we would like to calculate measures such as the likelihood of hazardous system failure over the Press' mission life (say, a year of operation) for various models of the Press design, including models where one or more components fail. The probability that the Press reaches a state satisfying property ϕ within an *operation time* of T seconds can be calculated using PRISM to evaluate the following CSL property:

$$\texttt{P}_{=?}\ [\ \texttt{true}\ \ \texttt{U}_{<=T/clock}\ \ \phi\ ]$$

In what follows we let $P(H_i, T)$ stand for the probability of hazard H_i arising in T seconds ($1 \leq i \leq 4$): e.g.

$$P(H_1, T) \stackrel{def}{=} \texttt{P}_{=?}\ [\ \texttt{true}\ \ \texttt{U}_{<=T/clock}\ \ (\texttt{state=10})\ ]$$

This specifies the probability that hazard H_1 occurs within the first T seconds of operation. The probability of a hazard occurring is formalised as

$$P(H_{all}, T) \stackrel{def}{=} \texttt{P}_{=?}\ [\ \texttt{true}\ \ \texttt{U}_{<=T/clock}\ \ \texttt{hazard}\ ]$$

where

$$\texttt{hazard} \stackrel{def}{=} \texttt{(state=10 | state=11 | state=12 | state=13)}$$

In assessing risk hazards are usually weighted according to their severity but here we simply treat them all equally; thus $P(H_{all}, T)$ represents the risk of hazardous system failure in operation up to time T.

Ideally we want to calculate $P(H_i, 1yr)$ under different assumptions about sensor failure rates, say with a mean time to failure of 5 years each. As shown in Section 7.1.2 below, however, such calculations are not computationally feasible for our models. So instead we decompose the problem into two parts as follows:

- the *Immediate Failure Likelihood (IFL)* and
- the *Mean Time to Failure (MTTF)*

where "failure" refers to hazardous system failure in both cases.

Immediate Failure Likelihood is an estimate of how likely the component failure is to lead to a hazardous system failure in the short term, namely within 60 sec in what follows. We need to consider a non-zero time frame because of the continuous-time nature of CTCMs. We chose 60 sec because it is the length of typical operational cycle of the Press, but other times could have been used. The notion is defined more precisely in the next section, together with a method for calculating it.

Mean Time to Failure, on the other hand, is an estimate of the expected number of operational cycles the system completes before hazardous failure. For component failures that usually reveal themselves immediately or after a short delay, the result will be less than 1. But for failures which may stay hidden for some time after the component fails, and are only revealed when particular combinations of circumstances arise, the result can be greater than 1. Hidden failures can be particularly nasty because, although their likelihood may be low in a single operational cycle, they are in some sense "just waiting to happen". The fault propagation mechanisms involved are often subtle and difficult for the designer to anticipate because they involve unusual combinations of circumstances, so having a way of identifying their presence is very valuable. Section 6.3 below describes a method for using PRISM to calculate MTTF and discusses some of the issues involved.

6.2 Revealed failures and Immediate Failure Likelihood

We define the *Immediate Failure Likelihood* for a given sensor failure mode and hazard H_i to be

$$\text{IFL} \stackrel{def}{=} P_M(H_i, 60) \tag{2}$$

where M is the CTMC model with the particular sensor failure mode enabled and with a sensor failure rate of 1/60 sec. We show below that IFL is a reasonable estimate of the likelihood that hazardous system failure H_i occurs within 60 secs (one typical operational cycle) of the sensor failing.

We need to explain why we use a sensor failure rate of 1/60 sec in P_M. As shown in Section 4, a sensor failure can have different consequences depending on the phase of operation in which it occurs. In the absence of other information, it is reasonable to assume that a sensor failure is equally likely to occur any time during the operation cycle, and thereby to use a linear cumulative distribution function (CDF) for the probability of occurrence. However, because we are using a CTMC modelling framework, we must instead use the exponential CDF from formula (1) on page 17 and select a value for the sensor failure rate `sensorFail` to approximate the linear CDF. We show below that one per 60 sec gives a reasonable estimate.

First note that, if the failure is equally likely to take place at any time, then the probability that it occurs during a phase of operation that typically takes T sec would be $T/60$. We consider each phase of operation in turn and show that the above model gives a reasonable approximation to this figure. We use the notation from Section 5.2.

First consider the case where, apart from the sensor failure transition, only a single simple unit transition is enabled (e.g., `[motorOn] state=1 -> state'=2`). In this case the transition rate relation $R(s, .)$ is dominated by the unit rate ($1 \gg sensorFail = clock/60$), so $E(s) \approx 1$. The likelihood that the failure occurs in this case is $p(s, s') \approx sensorFail$, where s' is the state where the sensor has failed. More generally, when $R(s, .)$ is dominated by a single value $\eta \gg sensorFail$, then $E(s) \approx \eta$ and the probability that the failure occurs is approximately $sensorFail/\eta$. (Note also that the expected time spent in the pre-state is approximately $clock/\eta$, no matter which transition is taken.)

Now consider the case where the plunger is rising below PONR and all enabled unit transitions have been taken. Inspection by hand, or us-

ing the PRISM simulator, shows that $R(s,.)$ is dominated by the transition `[plAbovePONR] state=3 -> RisingR1:(state'=4)` that takes the plunger past PONR, with rate $RisingR1$. Since $RisingR1 = clock/\text{RTP} \gg sensorFail$, then $E(s) \approx RisingR1$ and the probability that the sensor fails in this case is approximately $sensorFail/RisingR1 = \text{RTP}/60$, as desired.

Similar calculations show that, for a plunger transition which is expected to take T seconds with $T \ll 60$, the probability that the sensor fails in that phase is approximately $T/60$, as desired.

The final case to consider is where the Press is open, waiting for the operator to push the button. In this case the push-button rate $PushRate = clock/54$ is close in value to $sensorFail$. That means there are two possible transitions from this state (the button can get pushed or the sensor can fail), each with approximately the same probability. Thus $E(s) \approx 2 \times sensorFail$ and the probability that the sensor fails is approximately 1/2. The linear CDF on the other hand gives 54/60 for the probability that the sensor fails during this phase of operation and we can see that the approximation is not very good. The trade-off in improving the approximation is to complicate the model. For the purposes of this paper, we have taken the approach of keeping the model relatively simple and readable, at the expense of some precision in this case.

Note also that the expected time spent in the Press-open state before the next transition occurs is $clock/E \approx clock/(2 \times sensorFail) = 30$ sec. Our failure models thus effectively simulate a shorter operational cycle time than desired. There seems to be no easy way to resolve this problem without substantially complicating the model. However, since we are only interested in estimating the *relative* effects of design changes, and are careful not to make assertions about absolute probabilities, we prefer to stick with a relatively simple model of components and interactions. This discussion does however illustrate some of the sometimes unanticipated timing interactions and subtleties of using CTMCs to model stochastic systems.

The final point to note is that the probability that the sensor actually fails in the first 60 sec is $Exp_{60}(60) = 0.63$. Our method of calculating IFL thus underestimates even this simple possibility. But again there seems to be no easy way to resolve this issue. In Section 7.2.2 below we perform a sensitivity analysis to show that, although the approximation can affect results (e.g., under-reading by as much as 37% in some cases), the Rough Order of Magnitude (ROM) is not affected. It is thus valid to use the results to investigate the relative effect of different design choices on the ROM of

hazardous failures.

In summary, using a sensor failure rate of 1 per 60 sec seems to give the fairest comparison of the immediate risk, since it makes the likelihood of occurrence of sensor failure closely proportional to the time spent in the various phases of operation, other than the Press-open phase. But it is important to note that IFL is only an approximation, and should not be regarded as an actual probability of failure.

6.3 Hidden failures and MTTF calculations

The second case of quantitative risk analysis formalised here relates to *hidden failures*. These are failures where the fault lies dormant and is only revealed when suitable co-effectors are present. (Race conditions can also play a part, when they result in sensor data being received late. These are discussed further in Section 6.5.1 below.)

To some extent, the likelihood of such failures is already taken into account in the IFL calculation described above. For example, if the PONR sensor fails high, then the system appears to behave normally, as long as the operator does not attempt to abort operation (represented by the coeffector whereby the button is released while the plunger is falling above the PONR). The likelihood of the latter (1 in 100) is taken into account in the operator model in Section 5.4. Thus the likelihood of this case occurring within 60 sec of the sensor failing is taken into account in the calculation of IFL above. However, the fault will not be revealed until the operator tries to abort operation, and only then will the system failure (H4 loss of abort) occur – quite possibly under precisely the circumstances when abort is actually needed for safety reasons.

To investigate such failures we used PRISM's *rewards mechanism* [14] to calculate the Mean Time to Failure (MTTF) for hazardous failures. We extend the model with a *reward matrix* which applies a transition reward of 1 unit each time the Press closes (i.e., when the transition from state 8 to state 1 in the plunger model occurs), representing completion of an operational cycle. Then the MTTF R is calculated by evaluating the following reachability reward property [8]:

$$R \stackrel{def}{=} \mathtt{R}_{=?}\ [\ \mathtt{F\ hazard}\ ] \tag{3}$$

In cases where the probability of *not* reaching a hazardous state approaches zero as time increases (e.g., if on any path a hazard can eventually be

reached), then R evaluates to a finite number representing the expected number of operational cycles completed before a hazard occurs.

Unlike $P(H, T)$ above, PRISM is able to estimate R in a reasonably short time for very low sensor failure rates, and independent of the mission time. This makes it attractive for use during model development and debugging. As it turns out however, when low sensor failure rates (such as one per 5 years) are used, we find that system failures are dominated by race conditions, and there is not much difference in calculated MTTF between the results for fault-free behaviour and behaviour when sensor faults may be present. (This may also be due in part to inaccuracies in the numerical analysis methods used. Such inaccuracies tend to accumulate in CTMC models when there are large differences in the rates involved in different transitions [11], such as in our case.)

Instead or relying on such results, we propose the following heuristic for determining whether a failure is revealed in the short term or more likely to stay hidden. Just as for IFL above, we set the sensor failure rate to one per 60 sec and evaluate R for each failure mode in turn. For failures which are likely to be revealed within one operational cycle, R will evaluate to less than 1.0. If R is finite but greater than 1, on the other hand, this indicates that the system is likely to keep operating, and fail hazardously at some later time, when the required coeffectors occur.

In this last case, the value of R can often be used to help determine which coeffector must be involved. If a single coeffector is involved, and it occurs with probability p per cycle ($p \ll 1$), then R will be approximately $1/p$. Thus for example, for the PONR sensor stuck high failure noted above, R is approximately 100 (see Section 7.2.3), which is the expected number of operational cycles before abort occurs. R thus gives a strong clue as to what coeffectors to investigate. When R is very high, however, it typically indicates that race conditions are the issue, and it is necessary instead to use the PRISM animator (or some other method) to discover what fault propagation mechanisms are involved.

The success of the approach depends however on the system not having non-hazardous long-term behaviours with non-zero probability, because in such cases R evaluates to infinity. For example, if there is a non-zero probability that the Press will get into a stuck open or stuck closed situation (such as after a button stuck low failure), then $R = \infty$ and this method cannot be used to estimate MTTF. Therefore, the approach does not handle the non-hazardous system failures F1 (stuck open), F2 (stuck closed)

and F3 (incorrect opening) from Table 2. But conversely, an infinite value of R for our models indicates that a cycle exists (i.e., the press gets stuck open or stuck closed), and the PRISM animator can be used to discover the failure mechanism that gives rise to it. It is not clear to what extent this phenomenon can be generalised to other models however, since it is seems to be more due to good luck than good modelling for the Press study.

In summary then, using formula (3) to calculate the mean time to hazardous failure for a sensor failure mode with failure rate 1/60 sec gives a useful heuristic for discovering hidden failures. But as usual with these kinds of calculations, the results need careful interpretation. They should not be interpreted as an accurate estimation of mean time to hazardous system failure.

6.4 Likelihood of hazardous system failure

Returning to the original problem, the challenge was to estimate the risk of hazardous failure over a mission time of 1 yr with sensor failure rates of 1 per 5 yr, say. For sensor failure modes that are most likely to be revealed in the short term (MTTF $\leq$ 1), the hazard risk likelihood is roughly the likelihood of sensor failure multiplied by IFL. (When IFL is small, the more likely outcome is a non-hazardous system failure in this case.) The likelihood of sensor failure is $Exp_{5yr}(1yr) \approx 0.18$ from formula (1) on page 17.

For hidden failures on the other hand (MTTF between 1 and say 1000), the hazard risk likelihood is simply the likelihood of sensor failure itself, since the fault condition remains in place until the coeffector occurs, and the latter can usually be assumed to occur at least once during the rest of the system's mission time.

In situations where system failures are dominated by race conditions, the situation lies somewhere between these two extremes. See Section 6.5.1 for more discussion.

6.5 Other remarks

Before turning to the results of our PRISM analysis, some further remarks about strengths and weaknesses of the approach are in order.

6.5.1 Race conditions in fault-free operation

The first remark concerns the presence of race conditions in our models, including our baseline "fault-free" model of Press operation. In many system states, a "fast" transition (such as involved in data transmission and/or processing) can be enabled at the same time as a "slow" transition (such as the plunger rising from the bottom to the PONR), with a non-zero probability that the slow transition will be taken first, or instead of, the fast transition. As a result, hazards can occur with non-zero probability even when all the components are functioning correctly.

For example, consider the system state immediately after a normal abort: i.e., `[releaseButton]` occurs while `state=7 & stateC=2 & stateOp=1`. In the first, much more common case, the sequence of subsequent events would be `[buttonR, turnMOn, motorOn]`, resulting in `state=9` and successful abort. But an alternative sequence of events with non-zero probability is `[plBelowPONR, buttonR, turnMOn, motorOn]`, which results in `state=11` (hazard H2: dangerous motor activation). This corresponds to the case where the plunger passes PONR before the control system gets a chance to turn on the motor.

Although to some degree such behaviours are an artifact of the modelling approach used, they do in fact occur in real life, and should be taken into account in risk analysis and design for safety [39]. For this reason fault-free operation (i.e., without sensor failures) is also included in the analysis below. We note in passing that the methods discussed in this paper can be applied without considering sensor-update race conditions if desired, by tweaking the models to give "internal" controller actions priority over other actions. This is the approach taken in Grunske *et al* [24] for example.

6.5.2 Modelling non-hazardous system failures

As noted above, PRISM uses CSL as the formal language in which properties of CTMCs are formulated for model checking. The cause-consequence relation between component failure events and system hazards was easy to formulate in CSL because of the way we modelled component failure events as transitions (e.g. `tsFailsHigh`) and hazards as absorbing states (although, as remarked in Section 6.2, modelling of the timing of component failures presented issues).

One drawback of using CMTCs we encountered, however, was that we

could find no simple way to capture the non-hazardous system failures F1 (stuck open), F2 (stuck closed) and F3 (incorrect opening) in the model or in CSL. Part of the difficulty was due to the CTMC way of modelling timing indirectly using the exponential CDF and rates, and the need to specify a time frame over which probability is calculated. The fact that an event has not taken place within x sec does not imply that it will not take place within $x + \delta$ sec. We have not found a way of formulating F1–F3 in CSL, nor were we able to identify a suitable way of representing F1–F3 as absorbing states in the plunger model. We investigated PRISM's steady-state operator [8] as a possible solution, but calculating the probability of steady-state behaviour proved computationally infeasible for our model: the model checking process did not terminate.

As a result we have had to omit some of the sensor failure modes from our MTTF analysis below, as well as omitting F1–F3 from quantitative analysis more generally.

6.5.3 Other failure scenarios

As noted above, FMEA is typically conducted only for single component failures because of the difficulty of analysing system behaviour in the presence of multiple failures and the combinatorial complexity of considering all the different cases that arise [4]. One of the advantages of our approach is that to model multiple failures it is simply a matter of including versions of the sensor modules with the appropriate failure events enabled.

It is also straightforward to model a wide range of other failure scenarios such as common cause failures. For example, suppose it is found that the bottom sensor does not fail randomly but is in fact far more likely to fail when the plunger hits it. More specifically, suppose that the bottom sensor fails stuck high when the plunger reaches the bottom with probability 1 in 10,000. This could be modelled by adding the following transition to the bottom sensor module:

```
[bsFailsHigh] state=1 & !(stateBS=4 | stateBS=5 | stateBS=6)
                    -> bsFail: stateBS'=4;
```

with `bsFail = 0.0001`. In the rest of the paper however we focus primarily on risk associated with single sensor failures.

6.5.4 PRISM settings

In the results reported below we used the Gauss-Seidel iteration setting with termination epsilon set to 1E-6. This is an iterative numerical solution method, so 100% accuracy cannot be assumed, especially in computations which converge slowly (such as for high non-infinite values of reward R and low non-zero values of IFL) because of cumulative rounding errors [11]. PRISM provides steady-state detection by default, which in many cases considerably shortens computation time through use of approximation to predict convergence. In our modelling and analysis, however, we needed to deactivate this facility since it gave misleading results in some cases.

All our experiments were performed on a standard PC with an Intel Pentium 4 CPU 3GHz processor with Ubuntu 7.10 Linux as operating system. Probability results are rounded to two significant figures in the results below.

7 Results for the initial design of the Press

This section reports the results of our calculation of Immediate Failure Likelihood (IFL) and Mean Time To Failure (MTTF) for the Press system as modelled in Section 5, for normal "fault-free" operation and for the effects of individual sensor failure modes. It also reports on computation time and various sensitivity analyses along the way to establishing a baseline reference model against which the effects of different design decisions will be evaluated in later sections.

7.1 Fault-free operation

We first consider the case where sensors function correctly. Hazards can sometimes arise under these circumstances due to race conditions, as discussed in Section 6.5.1. Using the PRISM animator we found the following examples of how race conditions could give rise to each of the hazards from Table 4:

H1 (uncommanded closing) could occur if the operator pushes the button while the Press is open and then releases it again while the control system is turning the motor off but before the plunger has dropped below the top sensor.

H2 (dangerous motor activation) could occur if the plunger falls past PONR while the control system is turning the motor on after an abort.

H3 (unexpected closing) could arise if the Press closes as usual but there is a long delay before the controller receives the `plNotAtTop` signal, with the result that if the controller detects the button pushed signal while the Press is reopening, then it will erroneously turn the motor off while the plunger is rising.

H4 (abort fails) could occur if the plunger falls past PONR before the system is able to turn the motor on after an abort.

By selecting a suitably fast clock rate, these race conditions have very low probability, as shown below.

7.1.1 Effect of clock rate

The speed with which the control system receives and acts on signals from the sensors has a large effect on the likelihood that race conditions occur. The faster the clock rate, the more likely it is that the control system will react in time and carry out the intended operation of the Press.

To illustrate this, consider the H2-after-abort scenario described in Section 6.5.1 above. From the state in which the scenario begins, the probability of taking the `[plBelowPONR]` transition rather than the `[buttonR]` transition is roughly $Exp_{TTP}(clock)$. (The PRISM simulator is excellent for studying such scenarios step by step.) When $clock = 0.001$ this probability is 0.0011, and when $clock = 0.0001$ it is 0.00011 (rounded to two significant figures): i.e., an order of magnitude improvement.

Clock rate	$P(H_{all}, 60)$	**Comp. time**
1E-2	9.2 E-03	1.3
1E-3	1.1 E-03	11
1E-4	1.1 E-04	109
1E-5	1.1 E-05	1080

Table 7: IFL results for fault-free operation, for different clock rates

Table 7 shows the Immediate Failure Likelihood results for different clock rates, together with the PRISM computation time (in seconds). As can

be seen, the probability of any of the hazards occurring decreases roughly linearly with clock rate, whereas the computation time increases roughly linearly.

Clock rate	R (# operations)	**Comp. time**
1E-3	845	14
1E-4	7,582	70
1E-5	39,845	183
1E-6	69,444	244

Table 8: MTTF results for fault-free operation, for different clock rates

Table 8 shows the effect of different clock rates on MTTF, measured as expected number R of completed operational cycles before hazardous failure. Note that R increases as the clock rate gets faster, since the likelihood of unusual race conditions decreases, as anticipated. In fact, R is roughly inversely proportional to $P(H_{all}, 60)$. Another point to note is that the computation time for R is much less affected by the clock rate than was the computation time for $P(H_{all}, 60)$, which suggests that the MTTF approach scales better than the IFL approach.

Because the purpose of this paper is to explore the potential benefits and limitations of stochastic model checking, in what follows we have chosen to focus primarily on a clock rate of 1E-4 per sec: i.e., a unit transition has an expected duration of 0.0001 sec. The resulting computation time makes for reasonable turnaround time in experiments. In reality however, a higher-performance system architecture would probably be chosen for the Press, using a suitably fast processor, sensors and actuators. Unless explicitly stated otherwise, 1E-4 per sec is used as the default clock rate below.

7.1.2 Effect of operation time

Table 9 shows the effect of varying the operation time T (given in seconds), broken down by the different hazards. We consider an operation time T corresponding to 1-4 typical operational cycles, respectively. The likelihood of a hazard occurring within T seconds rises roughly linearly with the operation time, as we would expect. The longer we observe the system, the more likely the occurrence of a hazard becomes. Likewise, the computation time (given in seconds) rises roughly linearly with the operation time. One implication

T	$P(H_{all}, T)$	$P(H_1, T)$	$P(H_2, T)$	$P(H_3, T)$	$P(H_4, T)$	**Comp. time**
60	1.1 E-04	2.2 E-06	1.0 E-04	1.5 E-09	3.1 E-06	115 - 149
120	2.3 E-04	4.0 E-06	2.2 E-04	3.2 E-09	6.4 E-06	220 - 283
180	3.5 E-04	5.9 E-06	3.3 E-04	4.8 E-09	9.8 E-06	327 - 428
240	4.6 E-04	7.8 E-06	4.4 E-04	6.4 E-09	1.3 E-05	434 - 564

Table 9: Probability of hazard arising in first T seconds of fault-free operation

of the latter observation is that the extent to which it is feasible to use this approach for calculating risk of failure over a longer time period is very limited. It would not be feasible to use it to calculate risk over the system's mission lifetime (say $T = 1yr$), for example.

Although there is theoretically no limit specified for the value of T, in practice the maximum value to be chosen depends on the model in question and how long the user is willing to wait for results. For high values of T the accuracy of results can also be degraded due to approximations used in floating point arithmetic.

7.2 Failure Modes and Effects Analysis

This section summarises and discusses the results of model checking for each of the sensor failure modes. In what follows we assume we are working with a model M in which a single sensor failure is enabled.

7.2.1 Immediate Failure Likelihood

Table 10 shows the IFL results for the different sensor failure modes. The results for fault-free operation are also included for comparison. The computation time for the failure-mode experiments is of the order of 300-700 seconds. The boldface entries indicate the sensor failure modes that lead to substantially increased hazard risk over fault-free operation.

The results provide valuable insights into the relative likelihood of the different scenarios. The boldface cases correspond closely to the hazardous cause-consequence relationships revealed in Table 3 on page 15 (with the additional remarks in Section 4.3). Some of these cases are discussed in more detail below. The cases where the hazard probabilities in the presence of

Failure mode		$\mathbf{P(H_{all}, 60)}$	$\mathbf{P(H_1, 60)}$	$\mathbf{P(H_2, 60)}$	$\mathbf{P(H_3, 60)}$	$\mathbf{P(H_4, 60)}$
None		1.1 E-4	2.2 E-6	1.0 E-4	1.5 E-9	3.1 E-6
Button stuck	high	**6.3 E-1**	**6.3 E-1**	6.2 E-5	9.4 E-10	**1.6E-4**
	low	6.8 E-5	1.5 E-6	6.4 E-5	9.4 E-10	1.9 E-6
Bottom stuck	high	**6.5 E-2**	4.9 E-6	**2.1 E-3**	**6.2 E-2**	1.9 E-6
	low	9.8 E-5	1.7 E-6	9.4 E-5	9.4 E-10	2.8 E-6
Top stuck	high	**1.7 E-1**	1.7 E-6	9.7 E-5	**1.7 E-1**	2.9 E-6
	low	6.8 E-5	1.5 E-6	6.4 E-5	9.4 E-10	1.9 E-6
PONR stuck	high	**3.5 E-3**	2.2 E-6	6.2 E-5	1.5 E-9	**3.5 E-3**
	low	**1.6 E-1**	2.0 E-6	**1.6 E-1**	1.5 E-9	2.9 E-6

Table 10: IFL results for Press with initial design

sensor failures are less than for fault-free operation correspond to the cases where non-hazardous system failures are the more likely outcome.

Some of the inaccuracies due to the approximations used in calculating IFL noted in Section 6.2 become evident here. For example, if the button sensor is equally likely to fail high at any time during an operational cycle of the Press, then its likelihood of failing while the Press is open is about 54/60; this case will lead immediately to hazard H1 (uncommanded closing). In fact, H1 is the most likely outcome in all cases of this failure mode, other than when it fails while falling above PONR and the user aborts, in which case H4 will occur instead. The actual probability of H1 should thus be close to 1 for this case, whereas the IFL calculation gives a likelihood of 0.63. The difference is due to the possibility that the sensor may not fail at all withint the first 60 sec.

Perhaps the most surprising result is that H3 (unexpected closing) is quite likely to occur if the bottom sensor fails high. The Modelica model simply predicted that the Press would get stuck open in this case. Further reflection (and using PRISM's animator) reveals the following race-condition scenario under which H3 can occur: The Press starts closing as usual (event `plNotATTop`) but before the controller receives and acts on the top-sensor low signal (event `tsLow`), it instead thinks the Press is closed (because `bs=1`) and so turns the motor on, resulting in the plunger passing through states 7 and 9 to 4 as though closing was being aborted; but then finally the controller reacts to `tsLow` and turns the motor off, resulting in H3. This is a good example of how model checking can reveal hazardous behaviours that could

otherwise easily be overlooked.

Returning to the main conclusions to be drawn from Table 10, it is evident that this design for the control system is not robust against sensor failures, and that the safety of the Press system relies to too great a degree on the reliability of the individual sensors. One way of mitigating this in design would be to use replicated sensors (e.g., triple modular redundancy [6]). Another way would be to use fault tolerant design techniques in the control logic design. In Section 8 we modify the logic to add extra guards on critical transitions, such as checking for infeasible sensor signal combinations and failing safe if detected. We then repeat stochastic analysis to see how well the new design mitigates hazards.

7.2.2 Effects of time of occurrence of component failure

As noted in Section 6.2, the phase of operation during which a sensor fails can have a critical effect on the outcome. This section examines the sensitivity of IFL results to the choice of sensor failure rate `sensorFail`. The IFL calculations in most of this paper use a constant rate of once per 60 sec in order to approximate the case where the failure is equally likely to occur anytime in a typical operational cycle. This section considers how IFL is affected by this choice of rate. We also contrast it with the case where the failure is present from the start of operation.

PRISM uses exponential function of formula (1) to model the Cumulative Distribution Function (CDF) for probability of a transition being taken. Figure 8 shows Exp_X for different values of X (30, 60 and 90 sec), together with the linear CDF c. The first thing to note is that exponential CDF Exp_{60} underestimates the probability that a failure will occur at all within the first operational cycle by about 37% compared to the linear CDF ($Exp_{60}(60) = 0.63$, which explains the result of $P(H_1, 60) = 0.63$ in the case where the Button is stuck high as shown in Section 7.2.1).

Table 11 compares the results returned by PRISM for the different cases of single sensor failure modes and different failure occurrence-time models. The column marked 'from start' represents the case where the failure is present from the start of operation.

As can be seen, the occurrence-time model has a large effect on the hazard likelihood in most cases. In the case where the failure is present from the start of operation, some sensor failures do not lead to hazards at all. For example, if the button sensor is stuck low, then the Press simply fails open.

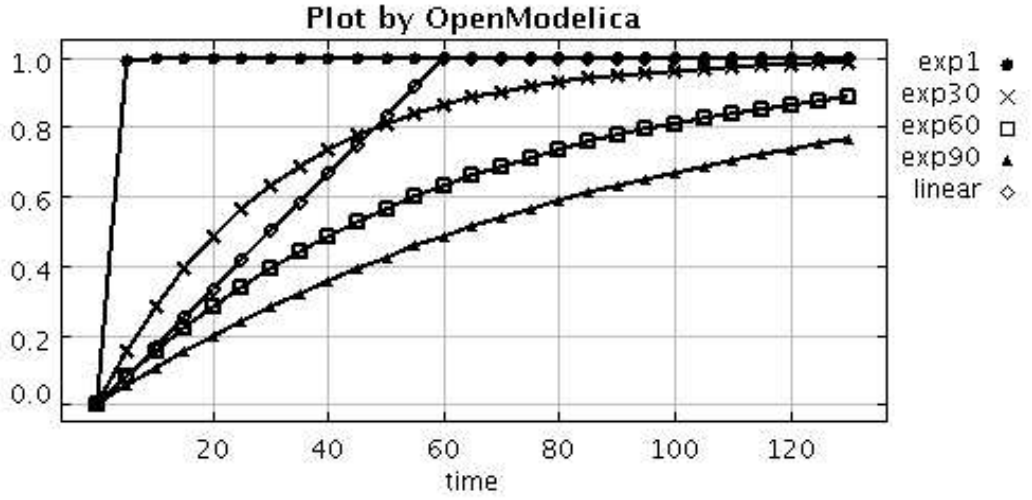

Figure 8: Some models of CDF for time of failure occurrence in operational cycle

Using the 'from start' model of sensor failure thus completely overlooks the case where the button sensor fails low during closing, which could in turn lead to hazard H4 (abort fails). In the case of the button being stuck high, Exp_{30}, representing behaviour where the failure is more likely to occur early in the operational cycle (expected time = 30 sec), gives a higher estimate of risk than Exp_{60}, where the failure is likely to occur later in the operational cycle. If the button is likely to fail early in the cycle then hazard H1 is more likely to occur. On the other hand, Exp_{30} leads to a lower estimate in the button stuck low case than Exp_{60} because an early occurrence of this failure leads to the Press failing open rather than a hazard.

But the important thing to note is that the rough order of magnitude (ROM) is the same in each case other than the 'from start' case. As argued in Section 6.2 above, using a sensor failure rate of one per 60 sec to calculate IFL is the most reasonable compromise.

7.2.3 Mean Time To Failure

Table 12 shows the Mean Time To Failure for hazardous failures, as explained in Section 6.3. The result was ∞ for the cases that are missing from the table (button, bottom and top sensor stuck low): in such cases there are non-

Model: Failure mode	$\mathbf{Exp_1}$	$\mathbf{Exp_{30}}$	$\mathbf{Exp_{60}}$	$\mathbf{Exp_{90}}$	from start
Button stuck high	1.0 E+0	8.6 E-1	6.3 E-1	4.8 E-1	1.0 E+0
Button stuck low	3.3 E-7	4.5 E-5	6.8 E-5	7.9 E-5	0.0 E+0
Bottom stuck high	1.6 E-1	9.9 E-2	6.5 E-2	4.8 E-2	1.6 E-1
Bottom stuck low	7.5 E-5	9.2 E-5	9.8 E-5	1.0 E-4	3.7 E-5
Top stuck high	4.3 E-1	2.6 E-1	1.7 E-1	1.3 E-1	4.4 E-1
Top stuck low	3.3 E-7	4.5 E-5	6.8 E-5	7.9 E-5	0.0 E+0
PONR stuck high	8.8 E-3	5.4 E-3	3.5 E-3	2.6 E-3	8.8 E-3
PONR stuck low	3.8 E-1	2.4 E-1	1.6 E-1	1.2 E-1	3.8 E-1

Table 11: Sensitivity of $P_M(H_{all}, 60)$ to models for time of failure occurrence in cycle

Sensor MTTF	1 min	10 min	100 min	5 yr
Fault-free operation	7,581			
Button stuck high	0.9	10	98	7,560
Bottom stuck high	0.9	10	98	7,560
Top stuck high	2.8	12	100	7,560
PONR stuck high	102	111	199	7,560
PONR stuck low	1.9	11	99	7,560
Comp. time (secs)	2-7	3-7	8-12	145-211

Table 12: MTTF for initial design measured in number of cycles, with different sensor reliability values

hazardous long-term behaviours with non-zero probability, such as when the Press gets stuck open or stuck closed.

The MTTF figures in Table 12 have been calculated for different sensor reliability values, namely, mean times to sensor failure of 1 minute, 10 minutes, 100 minutes and 5 years (the target value for our overall risk analysis). For the moment however we focus on the 1 min case since we use it to identify hidden failures, as discussed in Section 6.3.

As anticipated from the preliminary hazard analysis in Table 3 in Section 4, the 'button sensor stuck high' failure leads almost immediately to a hazardous system failure. This is confirmed by the result that, with a sensor failure rate of 1 per 60 sec, the expected time to system failure is also approx-

imately 1 operational cycle. (Likewise when the sensor MTTF is increased to 10 min then the system MTTF increases to 10 cycles, as expected.)

By contrast, system failures typically take longer to occur in the case 'top sensor stuck high' and the two PONR sensor failures, confirming that they are hidden failures. The result for the case 'PONR sensor stuck high' is 102, which is consistent with the fact that the operator typically aborts operation in only 1 in 100 cycles. Likewise, the coeffector for the 'PONR sensor stuck low' hazardous case is that the operator releases the button after PONR but before the Press fully closes, which we have assumed happens 50% of the time; hence a MTTF of approximately 2. As discussed in Section 6.3, the value of MTTF in both these cases gives a strong hint as to which coeffector is involved.

The 'top sensor stuck high' case is perhaps the most surprising result. The coeffector noted in Table 3 is that the button gets pressed while the Press is opening, which has low probability in our model (roughly $Exp_{54}(4) = 0.07$) and thus might be expected to lead to an MTTF ≈ 14. The calculated MTTF is roughly 3 operational cycles instead. The reason is that there are abort-like cycles with small but non-zero probability in the CTMC model which end in hazards but which get zero reward. These cycles drag down the calculated MTTF value. (For similar reasons it is important to note that MTTF < 1 does not imply hidden failures are not possible. They may simply be outweighed by the possibility of non-hazardous failures on other branches.)

It is interesting to note why the 'bottom sensor stuck high' case yields a non-infinite reward, despite leading to the Press becoming stuck open in the Modelica experiment in Section 4. Closer inspection reveals that the motor will actually turn off momentarily if the operator pushes the button and immediately turn back on. This "window of opportunity" opens the possibility of a hazard occurring, as discussed in Section 7.2.1, and this in turn enables a reward to be calculated for paths beyond such a point. The reward is giving a measure for such cases (which will be zero, if the Press doesn't close before the hazard occurs). In effect the fact that the calculated overall reward is less than 1 says that, if a hazardous behaviour is going to result, then the expected time is "within the same operational cycle" as the sensor failure. Thus MTTF calculated this way gives at best an indirect hint at what coeffectors might be involved.

As a final remark, it is interesting to note the effect that sensor reliability values have on the mean time to hazardous failure. The results indicate that,

for relatively high sensor failure rates (say, once per hour or once per day), the above patterns of immediate system failure and hidden failures apply, but as sensor reliability increases then race conditions start to dominate. As noted above, once MTTF becomes very large however, their accuracy cannot be trusted due to cumulative error in the numerical solutions involved. The main value of calculating the expected reward for individual component failure modes is thus likely to be in the insights it yields about hidden failures, complementary to what IFL reveals about criticality of component failures over shorter time frames.

7.3 Multiple failures

We conducted an experiment to measure the effect on computation time when multiple failures are injected. As explained in Section 6.5.3 this can be achieved simply by enabling the appropriate failure transitions in the sensor modules in our model. Table 13 shows the results when faults were injected in the following order: bottom sensor stuck high; button sensor stuck high; PONR sensor stuck high; top sensor stuck high. The complexity of the model rose 2-3 fold each time a new fault was injected, and this was reflected in increases in computation time.

# failures	IFL (H_{all} case)	R with sensor MTTF = 1 min	R with sensor MTTF = 5 yr
0	109	68	68
1	392	4	161
2	1,047	7	362
3	2,940	17	844
4	7,802	71	2,126

Table 13: Computation time (sec) for multiple failures

7.4 Summary and discussion

The analysis above indicates that the initial control system design is not sufficiently robust against sensor failures and race conditions. In fault-free operation (i.e., with the sensors functioning correctly) the presence of race conditions yields an Immediate Failure Likelihood of about 10^{-4}, mostly due

to hazard H2 (dangerous motor activation). This estimate clearly depends to a great degree on the stochasticity assumptions underlying the model, and in particular on the assumption that sensor-update timing failures are possible (and follow an exponential CDF rule). Nevertheless the analysis yields valuable insights into the relationship between race conditions and the clock rate, and suggests it would be better to use a faster clock rate than that used here (10^{-4} per sec), to reduce IFL to a more reasonable value (see Table 8). Section 9 explores another way of reducing the risk of hazard H2, by modifying the system design to move the PONR sensor slightly higher, which reduces the likelihood of the race condition.

Turning to FMEA, the deficiencies of the original (naive) control logic become even more apparent. Four of the sensor failure modes yield IFL probability estimates greater than 0.05, for example. That is, if a sensor fails in one of the given ways, then it is highly likely to lead to a hazard. Moreover, the MTTF calculations revealed that three of the sensor failure modes are hidden failures, and only require certain environmental conditions before they lead to hazardous system failures. Section 8 explores a way of modifying the control logic to make it more robust against sensor failures. We show that the change reduces the IFL of many of the sensor failure modes significantly (including two of the four critical modes) and almost eliminates the risk of hidden failures.

The analysis yielded insights into fault propagation mechanisms over and above those revealed by simulation (cf. Table 3). For example, in Section 7.2.1 we saw how a race condition could combine with the bottom sensor stuck high failure to give rise to hazard H3 (unexpected closing). The MTTF results gave good clues as to which coeffectors were involved in the hidden failure cases. Such insights can help the designer improve system design for safety.

8 Press with error-detecting control logic

The design change considered in this section is to modify the control logic to detect sensor failures where possible and fail safe [13]. We show that it is easy to modify the model and rerun the PRISM analysis to check if (and how well) the change mitigates hazard likelihood.

8.1 Modified control logic

We first modify the control logic to include all relevant sensor conditions in the guards, to avoid the problem noted in Section 7.2.1 above. Thus for example, rather than simply activating the motor drive when a 'bottom sensor high' signal is received, we shall also check that the PONR sensor signal is high and the top sensor signal is low. We also check for infeasible sensor value combinations, such as the top and bottom sensor signals being high simultaneously, and fail safe if such combinations are detected [13].

```
module Controller
  stateC : [1..4] init 1;
  ... // sensor value updates as before
  [turnMOn]  stateC=1 &
     ((bs=1 & ps=1 & ts=0)|(button=0 & ps=0 & bs=0)) -> stateC'=2;
  [] stateC=1 &
     (((bs=1|ps=1)& ts=1) | (bs=1 &(ps=0|ts=1))) -> stateC'=3;
  [turnMOff] stateC=2 & ts=1 & button=1 & ps=0 & bs=0 -> stateC'=1;
  [] stateC=2 &
     (((bs=1|ps=1)& ts=1) | (bs=1 &(ps=0|ts=1))) -> stateC'=4;
endmodule
```

Figure 9: Control logic revised to include error-detection

The revised control logic is shown in Figure 9. The rest of the model remains unchanged. The infeasible sensor value combinations are `(bs=1|ps=1) & ts=1` and `bs=1 & (ps=0|ts=1)`. If an infeasible sensor value combination is detected we simply fail safe by leaving the motor actuator in its current state. This is achieved by adding new states 3 and 4 to the Controller, corresponding to leaving the motor permanently off or on, respectively. Thus, if the failure is detected as the Press is closing, then the Press will be allowed to close but then remain closed thereafter. Similarly, if the failure is detected while the Press is opening or open, then the Press will be allowed to open fully and then remain open thereafter.

To calculate MTTF we modify the reward property of formula (3) to take the failed-safe states into account:

$$R' \stackrel{def}{=} \mathtt{R}_{=?}\ [\ \mathtt{F}\ (\mathtt{hazard} \mid \mathtt{stateC} = 3 \mid \mathtt{stateC} = 4)\ ]$$

Clock rate	Error-detecting Design		Initial Design	
	R' (# operations)	Comp. time	R (# operations)	Comp. time
1E-3	369	15	845	14
1E-4	3,512	81	7,582	70
1E-5	24,760	292	39,845	183
1E-6	62,778	492	69,444	244

Table 14: MTTF for fault-free Press with and without error detection, for different clock rates

The change is required since $R = \infty$ in the presence of the new reachable absorbing controller states 3 and 4.

8.2 Results: fault-free operation

Recall that, in the fault-free case for the initial Press control system design, it was the presence of race conditions that gave rise to hazards. For the most part those race conditions have not been addressed in the redesign, except for the one described in Section 7.2.1 above, whereby hazard H3 could arise if the control system was slow in detecting and acting on the 'top sensor signal low' condition. The particular combination of events that gave rise to this case has been eliminated in the redesign by instead failing safe if the top sensor value is still low when the bottom sensor value goes high. The reduced risk is confirmed by recalculating $P(H_3, 60)$: the result has dropped from 1.5E-9 in Table 10 to 3.3E-13 in Table 15 below. However, the other immediate-failure likelihood results are virtually unchanged for the fault-free case: the offending race conditions are still present.

Table 14 shows the effect the revised logic has on MTTF in the fault-free case. As perhaps expected, the revised Press has a slightly shorter MTTF due to higher likelihood of failing safe because of race conditions.

8.3 With sensor failures

Table 15 shows the Immediate Failure Likelihood results for each sensor failure mode if they diverge from the results for the original Press design as given in Table 10. Cases where the results are not (or only marginally)

Failure mode		$\mathbf{P(H_{all}, 60)}$	$\mathbf{P(H_1, 60)}$	$\mathbf{P(H_2, 60)}$	$\mathbf{P(H_3, 60)}$	$\mathbf{P(H_4, 60)}$
None		≈	≈	≈	3.3 E-13	≈
Button stuck	high	≈	≈	≈	3.5 E-13	≈
	low	≈	≈	≈	2.1 E-13	≈
Bottom stuck	high	**2.2 E-03**	1.4 E-06	≈	2.1 E-13	1.6 E-04
	low	≈	≈	≈	2.9 E-13	≈
Top stuck	high	**2.5 E-03**	≈	≈	**2.4 E-03**	≈
	low	≈	≈	≈	2.1 E-13	≈
PONR stuck	high	**2.2 E-04**	≈	≈	2.1 E-13	**1.6 E-04**
	low	≈	≈	**1.4 E-01**	2.9 E-13	≈

Table 15: Diverging results for IFL for Press using the error-detecting control logic

affected by the design change are indicated using the ≈ sign. The dominant failures that have changed are shown in boldface. As seen by comparing with Table 10, many of the dominant failures have been mitigated significantly. For example, the likelihood that 'bottom sensor stuck high' leads to H3, as described in Section 7.2.1, has all but been eliminated (reduced from 6.2E-2 to 2.1E-13). The likelihood that 'top sensor stuck high' leads to H3 has been reduced by two orders of magnitude (from 1.7E-1 to 2.4E-3), and the likelihood that 'PONR sensor stuck high' leads to H4 has been reduced by an order of magnitude (from 3.5E-3 to 1.6E-4).

However, the design modification has had very little effect on the likelihood that 'PONR sensor stuck low' leads to H2, and no effect on the likelihood that 'button sensor stuck high' leads to H1 (which is not surprising, because we cannot detect button failures this way). The likelihood that 'bottom sensor stuck high' leads to H4 has actually increased (from 1.9E-6 to 1.6E-4), but this is probably a small anomaly due to the likelihood of getting stuck open being reduced in the new design.

Table 16 shows the Mean Time To Failure (in expected number of operational cycles completed) for hazardous and fail-safe failures in the case of different sensor reliability values, and gives the corresponding results for the initial design from Table 12 for comparison. The result was ∞ in the sensor failure-mode cases not shown in the table. As discussed in Section 6.3, these are cases where the press gets stuck open or stuck closed but without entering a fail-safe state.

	Error-detecting Design			Initial Design		
Fault-free operation	3,511			7,581		
Sensor MTTF	**1 min**	**10 min**	**5 yr**	**1 min**	**10 min**	**5 yr**
Button stuck high	0.9	9.6	3,507	0.9	10	7,580
Bottom stuck high	0.9	9.9	3,507	0.9	10	7,560
Top stuck high	0.9	9.9	3,507	2.8	12	7,560
PONR stuck high	0.9	9.9	3,507	102	111	7,560
PONR stuck low	1.4	10.4	3,507	1.9	11	7,560
Comp. time (secs)	3-6	5-7	190-216	2-7	3-7	145-211

Table 16: MTTF for Press design with and without error detection, for different sensor MTTF values

As can be seen from Table 16, the risk of failures remaining hidden has been significantly mitigated by the revised control logic. Both 'top stuck high' and 'PONR stuck high' now have expectation of being revealed within one operational cycle. 'PONR stuck low' is revealed when the plunger hits bottom, which counts as completion of an operational cycle and explains why MTTF is greater than 1 in its case.

8.4 Summary and discussion

Modifying the control logic has had a very beneficial effect, in terms of significantly reducing the risk of hidden failures, as well as significantly reducing the likelihood of the race condition discussed in Section 7.2.1 above. Of the remaining risks, the dominant failures are 'button sensor stuck high' leading to H1 (uncommanded closing) and 'PONR sensor stuck low' leading to H2 (dangerous motor activation).

There are several different ways that the 'button sensor stuck high' failure could be mitigated in the design. One way would be to reduce the severity of the failure by introducing a means for detecting if anyone is in the vicinity of the Press (such as infrared detection), and preventing closing in such a case. This would of course also involve moving the button location to outside of the danger zone. Another solution would be to introduce a second button, and to require that both buttons be pushed before the motor would switch off [12]. Yet another solution would be to check that the button signal is low

when the plunger reaches the top and fail safe otherwise. This would involve a change to the operational procedure so that the operator was required to release the button before the plunger reaches the top.

All of these solutions can be modelled in our framework. To demonstrate, we focus on the 'PONR sensor stuck low' failure mode and show how stochastic model checking can further inform design-for-safety. The next section investigates the effect of raising the PONR sensor above its nominal position, in order to reduce the likelihood of the race condition that leads to H2 during fault-free operation.

9 Raising the Point of No Return sensor

The second design change we consider involves moving the PONR sensor higher, in order to reduce the effect of the race condition that led to the motor drive being activated late (hazard H2) in fault-free operation.

9.1 Modified sensor layout

We modify the Press design so that the PONR sensor is raised higher than the plunger's actual (physical) point of no return. This way, if there is a delay in activating the motor drive after a late abort, the delay will hopefully be absorbed while the plunger is still falling above the physical PONR, and the motor drive will be activated before the plunger reaches that point. We call the new PONR sensor position the *operational PONR* (i.e., the point after which it is no longer possible to abort closing) and denote its value by *oPONR* in what follows.

The modified design is modelled by tweaking the model from Section 8 (see Figure 10). States 3, 4 and 7 are now interpreted as rising below, rising above and falling above oPONR, respectively. The state "falling below oPONR" is split into state 8 (falling below PONR) and new state 14 (falling between oPONR and PONR). States 9 and 15 represent the plunger state after the motor drive is activated in states 7 and 14 respectively. In both cases the plunger's fall will be slowed – without reaching the bottom – and then reversed, and the plunger will eventually move into state 4 as before. The hazards are defined as before.

In the PRISM code we achieve this by replacing transition

```
[plBelowPONR] state=7 & stateOp=2 -> FallingR1:(state'=8);
```

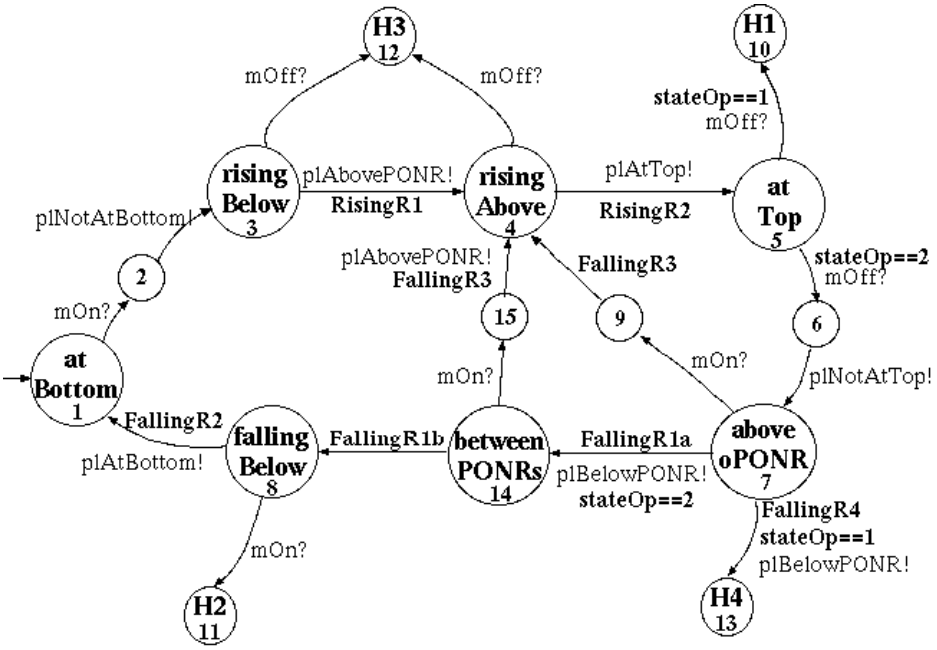

Figure 10: Behaviour of plunger with raised PONR sensor

in the plunger module with

```
[plBelowPONR] state=7 & stateOp=2 -> FallingR1a:(state'=14);
[]            state=14 -> FallingR1b:(state'=8);
```

and adding transitions

```
[motorOn]     state=14 -> state'=15;
[plAbovePONR] state=15 -> FallingR3:(state'=4);
```

We set `FallingR1a = clock/TTOP` and `FallingR1b = clock/(TTP-TTOP)` where *Time To Operational PONR (TTOP)* is the time it normally takes the plunger to fall to oPONR. Note that events `plAbovePONR` and `plBelowPONR` in the revised model are triggered by the plunger passing the PONR sensor, and thus occur at oPONR rather than PONR. Strictly speaking we should change the values of rate `RisingR1` and `Rising R2`, but the change is too small to affect the results significantly.

In what follows we report results for two different cases: one where the PONR sensor is raised only slightly (to 1.5m from 1.44m, with TTOP=1.773) and the other where it is raised significantly (to 5.25m, with TTOP=1.0).

	$\mathbf{P(H_{all}, 60)}$	$\mathbf{P(H_1, 60)}$	$\mathbf{P(H_2, 60)}$	$\mathbf{P(H_3, 60)}$	$\mathbf{P(H_4, 60)}$	**Comp. time (sec)**
D1	1.1 E-04	2.2 E-06	1.0 E-04	1.5 E-09	3.1 E-06	109-140
D2	1.1 E-04	2.2 E-06	1.0 E-04	3.3 E-13	3.1 E-06	244-304
D3	6.7 E-06	2.2 E-06	1.5 E-06	3.3 E-13	3.1 E-06	294-360
D4	4.1 E-06	2.2 E-06	1.4 E-07	3.3 E-13	1.8 E-06	272-334

Table 17: IFL for fault-free operation for different Press designs: (D1) initial design; (D2) with error detection; (D3) with PONR raised to 1.5m; (D4) with PONR raised to 5.25m

The Modelica model was used to derive the values of height of oPONR and TTOP.

9.2 Results: fault-free operation

Table 17 shows the Immediate Failure Likelihood for fault-free operation for the revised design for the two different oPONR heights. The corresponding results for the initial design, with and without error detection are given for comparison. As can be seen, raising the PONR sensor reduces the IFL of dangerous motor activation (hazard H2) by 2-3 orders of magnitude in fault-free operation, without increasing the likelihood of the other hazards. Table 18 also shows marked improvement in the long-term risk of H2, confirming that raising the PONR sensor significantly reduces the likelihood of the main race condition that gave rise to H2, without introducing new hidden failures.

9.3 With sensor failures

Although raising the PONR sensor improves safety in the fault-free case, it has little or no effect on the IFL results in the cases where sensors may fail. The results are so similar to those in Table 15 above that they are not given here. In almost every case they are the same as, or slightly lower than, the results for the error-detecting design in Section 8. The only exception is that the likelihood of H2 increases from 2.1E-3 to 9.1E-3 in the "bottom sensor stuck high" case when TTOP=1, which is probably due to reduced likelihood

	Error-detecting		Raised PONR TTOP=1.773		Raised PONR TTOP=1	
	Fault-free	Sensor MTTF=5yr	Fault-free	Sensor MTTF=5yr	Fault-free	Sensor MTTF=5yr
MTTF	3,511	3,507	16,404	16,304	14,882	14,799
Comp. time	82	190-216	263	598-685	242	583-656

Table 18: MTTF for three different Press designs, for fault-free and fault-prone operation

of some of the hazards that would normally precede the H2 case.

Likewise, the MTTF results are almost identical to those for the error-detecting design given in Table 16, at least for the relatively low values of sensor reliability (1–100 mins). As seen from Table 18 above however, for higher values of sensor reliability (in this case, 5yrs) the revised design has a longer meant time to hazardous failure, due to reduction of risk due to the race condition around the time the plunger passes the PONR.

10 Summary and Conclusions

The paper presented an approach to risk analysis using stochastic model checking – or more specifically, using Continuous Time Markov Chains (CTMC) models and the PRISM tool. The approach was illustrated on the Industrial Press case study. Although relatively simple, the Press exhibits a wide range of different behaviours, including hidden failures and subtle race conditions. We illustrated the use of quantitative analysis in support of Failure Modes and Effects Analysis – in this case, the effects of sensor failures on hazardous system behaviour.

Even with such a relatively simple system, a brute force computation of risk over a 1 year mission lifetime proved computationally infeasible. (This holds true for much shorter mission times also, such as for example in the case where a thorough inspection and test is carried out weekly.)

The main contribution of the paper was to provide computationally feasible methods for quantitative assessment of cause-consequence relations. Section 6 introduced two complementary analysis techniques: the first for estimating the likelihood of short-term failures (i.e., those which typically

manifest themselves within one operational cycle of the Press); and the second for identifying hidden failures (i.e., those which only manifest themselves only under specific sets of environmental conditions, which may themselves be comparatively rare). Together these two techniques yield valuable insights into which aspects of system design need more attention for safety. The short-term failure analysis method yields a quantitative relationship between component failures and their consequences at system level akin to a criticality measure. The heuristic for identifying hidden failures provides a good clue as to the conditions under which the hazard will arise, although subtle race conditions can sometimes confound the situation.

Our system models were based on CTMC models derived almost directly from the operational concept for the system. (A Modelica simulation was used to derive values for key rates in the model.) We demonstrated an approach to injecting faults directly into a CTMC model of the system. This has the advantage of facilitating analysis of changes to system design simply and quickly, and of deriving consequences of component failures directly from the model. This contrasts with most other forms of FMEA and criticality analysis, whereby models of fault propagation are constructed or generated separately and then have quantitative analysis performed on them. Our approach is more agile and more directly aligned with the system development process, since it does not require new fault propagation models to be constructed when the system model changes. We also included the possibility of sensor-update timing failures (one of the sources of race conditions in our model) and investigated the effect of data processing rates on hazard likelihood.

One downside of the approach to fault injection is that it may alter some of the stochastic properties of the system model being studied (cf. Section 6.2). Through careful mathematical analysis and sensitivity analysis experiments we showed that the side-effects are relatively minor in our case study, and that the order of magnitude of probability estimates is not affected. It remains an open question however to what degree this approach generalises to other systems. We anticipate that the kind of argument given in Section 6.2 would transfer to most systems with natural "cycles of operation" (such as many manufacturing systems).

Another unanticipated difficulty we encountered was not being able to express some of the interesting system properties in CSL. As well as limiting the kinds of properties for which Immediate Failure Likelihood could be calculated, it also prevented detection of hidden failures in cases where such

behaviours had non-zero probability.

The paper is rare in presenting a detailed study of the possibilities and challenges of stochastic model checking for safety related systems. We show that CTMCs are a reasonably natural way of modelling system behaviour and component failures, and that the PRISM approach has some very useful features for assisting in quantitative risk analysis.

At the same time, however, CTMCs provide challenges in representing the timing behaviour of the system accurately. For future work it would be interesting to investigate how other models of stochastic processes compare, such as Probabilistic Timed Automata (which separate the notion of probability from that of timing) [40] or Interactive Markov Chains [41] (which allow probabilistic transitions as well as non-deterministic choices between transitions). At the moment, however, the tool support for these notation is not as advanced as that for CTMCs.

The PRISM simulator was very helpful for debugging our models and discovering the scenarios under which component failures led to system failures, and the fault propagation mechanisms involved. Counterexample visualization [25] is a promising technology that could improve the analyst's ability to determine which fault propagation mechanisms contribute most significantly to risk. It would be interesting to see if the approach could be extended to our method for calculating mean time to failure, to improve the analyst's ability to determine which fault propagation mechanisms are involved in hidden failures.

Acknowledgements

The authors gratefully acknowledge the assistance with PRISM and Modelica provided by David Parker and Adrian Pop respectively. This research was carried out through the ARC Centre for Complex Systems with funding from the Australian Research Council.

References

[1] N. G. Leveson, Safeware: System Safety and Computers, Addison-Wesley, 1995.

[2] N. Storey, Safety-Critical Computer Systems, Addison-Wesley, 1996.

[3] International Electrotechnical Commission, Functional Safety of Electrical/Electronic/Programmable Electronic Safety-Related Systems, International Standard IEC 61508 (1998).

[4] International Electrotechnical Commission, Analysis Techniques for System Reliability – Procedure for Failure Mode and Effect Analysis (FMEA), International Standard IEC 60812 (1985).

[5] E. J. Henley, H. Kumamoto, Probabilistic Risk Assessment: Reliability Engineering, Design, and Analysis, IEEE Press, 1992.

[6] D. Smith, Reliability, Maintainability and Risk, 7th Edition, Elsevier Butterworth-Heinemann, Amsterdam, 2005.

[7] M. Kwiatkowska, G. Norman, D. Parker, PRISM: Probabilistic symbolic model checker, in: T. Field, P. Harrison, J. Bradley, U. Harder (Eds.), Proc. of Int. Conf. on Modelling Techniques and Tools for Computer Performance Evaluation (TOOLS'02), Vol. 2324 of LNCS, Springer, 2002, pp. 200–204.

[8] PRISM manual, http://www.prismmodelchecker.org/manual/.

[9] P. Fritzson, Principles of Object-Oriented Modeling and Simulation with Modelica 2.1, IEEE Press, 2004.

[10] C. Baier, J.-P. Katoen, H. Hermanns, Approximate symbolic model checking of Continuous Time Markov Chains, in: J. Baeten, S. Mauw (Eds.), Proc. Int. Conf. on Concurrency Theory (CONCUR'99), Vol. 1664 of LNCS, Springer, 1999, pp. 146–161.

[11] A. Reibman, K. Trivedi, Numerical transient analysis of Markov models, Computers & Operations Research 15 (1) (1988) 19–36.

[12] J. Hall, J. Jacob, J. McDermid, I. Toyn, Towards a z method: the two button press case study, Tech. rep. (May 1995).

[13] B. Atchison, P. Lindsay, Safety validation of embedded control software using Z animation, in: Proc 5th IEEE Int Symp on High Assurance Systems Engineering (HASE'00), IEEE, 2000, pp. 228–237.

[14] M. Kwiatkowska, G. Norman, D. Parker, Stochastic model checking, in: M. Bernardo, J. Hillston (Eds.), Formal Methods for the Design of Computer, Communication and Software Systems: Performance Evaluation (SFM'07), Vol. 4486 of LNCS (Tutorial Volume), Springer, 2007, pp. 220–270.

[15] C. J. Price, N. Taylor, Automated multiple failure FMEA, Reliability Engineering and System Safety 76 (1) (2002) 1–10.

[16] B. Atchison, P. Lindsay, D. Tombs, A case study in software safety assurance using formal methods, Tech. rep., University of Queensland, SVRC 99-31, `www.itee.uq.edu.au/~pal/SVRC/tr99-31.pdf` (1999).

[17] Y. Papadopoulos, D. Parker, C. Grante, A method and tool support for model-based semi-automated failure modes and effects analysis of engineering designs, in: Proc. 9th Australian Workshop on Safety Critical Systems and Software (SCS'04), Australian Computer Society, Inc., 2004, pp. 89–95.

[18] B. Kaiser, C. Gramlich, M. Förster, State/event fault trees – a safety analysis model for software-controlled systems, Reliability Engineering & System Safety 92 (11) (2007) 1521–1537.

[19] J. D. Reese, N. G. Leveson, Software deviation analysis, in: Proceedings of the 19th International Conference on Software Engineering, ACM Press, 1997, pp. 250–261.

[20] T. Cichocki, J. Górski, Failure mode and effect analysis for safety-critical systems with software components, in: F. Koornneef, M. van der Meulen (Eds.), Proc. of Int. Conf. on Computer Safety, Reliability and Security (SAFECOMP 2000), Vol. 1943 of LNCS, Springer, 2000, pp. 382–394.

[21] M. Bozzano, A. Villafiorita, Improving system reliability via model checking: The FSAP/NuSMV-SA safety analysis platform., in: Proc. of Int. Conference on Computer Safety, Reliability, and Security (SAFECOMP 2003), Vol. 2788 of LNCS, Springer, 2003, pp. 49–62.

[22] M. P. E. Heimdahl, Y. Choi, M. W. Whalen, Deviation analysis: A new use of model checking, Automated Software Engineering 12 (3) (2005) 321–347.

[23] L. Grunske, P. A. Lindsay, N. Yatapanage, K. Winter, An automated failure mode and effect analysis based on high-level design specification with Behavior Trees, in: J. Romijn, G. Smith, J. van de Pol (Eds.), Proc. of Int. Conf. on Integrated Formal Methods (IFM'05), Vol. 3771 of LNCS, Springer, 2005, pp. 129–149.

[24] L. Grunske, R. Colvin, K. Winter, Probabilistic model-checking support for FMEA, in: M. Harchol-Balter, M. Kwiatkowska, M. Telek (Eds.), Proc. of 4th Int. Conf. on the Quantitative Evaluation of SysTems (QEST 2007), IEEE Computer Society Press, 2007, pp. 119–128.

[25] H. Aljazzar, M. Fischer, L. Grunske, M. Kuntz, F. Leitner, S. Leue, Safety analysis of an airbag system using probabilistic FMEA and probabilistic counter examples, in: Proc. of Int. Conf. on the Quantitative Evaluation of SysTems (QEST 2009), IEEE Computer Society Press, 2009.

[26] J. Elmqvist, S. Nadjm-Tehrani, Formal support for quantitative analysis of residual risks in safety-critical systems, in: Proc. High Assurance Systems Engineering Symposium (HASE'08), IEEE Computer Society, 2008, pp. 154–164.

[27] A. D. Domínguez-Garca, J. G. Kassakian, J. E. Schindall, J. J. Zinchuk, An integrated methodology for the dynamic performance and reliability evaluation of fault-tolerant systems, Reliability Engineering & System Safety 93 (11) (2008) 1628–1649.

[28] M. Bozzano, A. Cimatti, J.-P. Katoen, V. Y. Nguyen, T. Noll, M. Roveri, The COMPASS approach: Correctness, modelling and performability of aerospace systems, in: Proc. 28th Int. Conf. on Computer Safety, Reliability and Security (SAFECOMP 2009), Vol. 5775 of LNCS, Springer, 2009, pp. 173–186.

[29] The MRMC model checker, `http://www.mrmc-tool.org/trac/`.

[30] O. Hasan, N. Abbasi, S. Tahar, Formal probabilistic analysis of stuck-at faults in reconfigurable memory arrays, in: M. Leuschel, H. Wehrheim (Eds.), Proc. of Int. Conf. on Integrated Formal Methods (IFM'07), Vol. 5423 of LNCS, Springer, 2007, pp. 277–291.

[31] J. P. Katoen, M. Khattri, I. S. Zapreev, A Markov Reward Model Checker, in: Proc. of Quantitative Evaluation of Systems (QEST 2005), IEEE Computer Science, 2005, pp. 243–244.

[32] H. Hermanns, J.-P. Katoen, J. Meyer-Kayser, M. Siegle, A markov chain model checker, in: Proc. of Int. Conf. on Tools and Algorithms for Construction and Analysis of Systems (TACAS 00), Vol. 1785 of LNCS, Springer-Verlag, 2000, pp. 347–362.

[33] K. Sen, M. Viswanathan, G. Agha, Statistical model checking of black-box probabilistic systems, in: Proceedings of Int. Conference on Computer Aided Verification (CAV '04), Vol. 3114 of LNCS, Springer, 2004, pp. 202–215.

[34] H. L. S. Younes, R. G. Simmons, Probabilistic verification of discrete event systems using acceptance sampling, in: Proceedings of the 14th International Conference on Computer Aided Verification (CAV '02), Vol. 2404 of LNCS, Springer-Verlag, 2002, pp. 223–235.

[35] D. N. Jansen, J. Katoen, M. Oldenkamp, M. Stoelinga, I. Zapreev, How fast and fat is your probabilistic model checker? an experimental performance comparison, in: Proceedings of the Haifa Verification Conference, Vol. 4899 of LNCS, Springer, 2007, pp. 69–85.

[36] H. Younes, M. Kwiatkowska, G. Norman, D. Parker, Numerical vs. statistical probabilistic model checking, Software Tools for Technology Transfer 8 (3) (2006) 216–228.

[37] D. D'Aprile, S. Donatelli, J. Sproston, CSL Model Checking for the GreatSPN Tool, in: T. Dayar, I. Korpeoglu (Eds.), Proc. of International Symposium on Computer and Information Sciences, Vol. 3280 of LNCS, Springer, 2004, pp. 543–552.

[38] E. Bode, M. Herbstritt, H. Hermanns, S. Johr, T. Peikenkamp, R. Pulungan, R. Wimmer, B. Becker, Compositional performability evaluation for STATEMATE, in: Proc. of Int. Conf. on the Quantitative Evaluation of SysTems (QEST 2006), IEEE Computer Society, 2006, pp. 167–178.

[39] F. Redmill, M. Chudleigh, J. Catmur, System Safety: HAZOP and Software HAZOP, John Wiley & Sons, 1999.

[40] M. Kwiatkowska, G. Norman, J. Sproston, F. Wang, Symbolic model checking for probabilistic timed automata, in: Y. Lakhnech, S. Yovine (Eds.), Proc. Joint Conference on Formal Modelling and Analysis of Timed Systems and Formal Techniques in Real-Time and Fault Tolerant Systems (FORMATS/FTRTFT'04), Vol. 3253 of LNCS, Springer, 2004, pp. 293–308.

[41] H. Hermanns, Interactive Markov Chains and the Quest for Quantified Quality, Vol. 2428 of LNCS, Springer, 2002.

A Modelica model of the Press

This is the model for normal (fault-free) operation of the Press:

```
class Press
    constant Integer M = 50;
    constant Integer H = 7;
    constant Integer F = 850;
    constant Real g = 9.81;
    constant Real Fr = 6.31;
    constant Real PONR = 1.44;

    Boolean userpushbutton;
    Real h, v;
    Boolean topsensor, bottomsensor, ponrsensor, buttonsensor;
    Integer motoron(start=2);

equation
    der(h) = v;
    when {h < 0, h > H} then reinit(v, 0); end when;
    der(v) =
        if motoron == 1 then
            if h < H then
                F/M-g + (if v>0 then -Fr else Fr)
            else 0
        else
            if h > 0 then
                -Press.g + (if v>0 then -Fr else Fr)
```

```
            else 0;

    topsensor =     h >= H;
    ponrsensor =    h <= PONR;
    bottomsensor =  h <= 0;
    buttonsensor =  userpushbutton;

    switchon = bottomsensor or
                (not buttonsensor and not ponrsensor);

    switchoff = topsensor and buttonsensor;

    motoron = if pre(motoron) == 2 and switchon then 1
                else if pre(motoron) == 1 and switchoff then 2
                else pre(motoron);
end Press;
```

Before executing the model it is necessary to add equations that describe the operator behaviour. For example, the case where the operator pushes the button after 58 sec and releases it again 3 sec later would be defined by:

```
    userpushbutton = if 58 < time < 61 then true else false;
```

To model the case where for example the top sensor fails stuck high from 5 sec into operation, the equation for `topsesnor` above would be replaced by:

```
    topsensor = if time < 5 then h >= H else true;
```

B Prism model

The following modules were omitted from Section 5 in the interests of space, so are included here for completeness.

```
module BottomSensor
    stateBS : [0..6] init 2;       // High(1), Low(3)
    [plAtBottom]    stateBS=0 -> stateBS'=1;
    [bsHigh]        stateBS=1 -> stateBS'=2;
    [plNotAtBottom] stateBS=2 -> stateBS'=3;
    [bsLow]         stateBS=3 -> stateBS'=0;
```

```
    [bsFailsHigh] !(stateBS=4 | stateBS=5 | stateBS=6)
        -> SensorFail: stateBS'=4;
    [bsHigh]      stateBS=4 -> stateBS'=6;
    [bsFailsLow]  !(stateBS=4 | stateBS=5 | stateBS=6)
        -> SensorFail: stateBS'=5;
    [bsLow]       stateBS=5 -> stateBS'=6;
    [plAtBottom]     stateBS=6 -> stateBS'=6;
    [plNotAtBottom]  stateBS=6 -> stateBS'=6;
endmodule

module PONRSensor
    statePS : [0..6] init 0;       // High(1), Low(3)
    [plAbovePONR] statePS=0 -> statePS'=1;
    [psLow]    statePS=1 -> statePS'=2;
    [plBelowPONR] statePS=2 -> statePS'=3;
    [psHigh]     statePS=3 -> statePS'=0;
    [psFailsHigh] !(statePS=4 | statePS=5 | statePS=6)
        -> SensorFail: statePS'=4;
    [psHigh]      statePS=4 -> statePS'=6;
    [psFailsLow]  !(statePS=4 | statePS=5 | statePS=6)
        -> SensorFail: statePS'=5;
    [psLow]       statePS=5 -> statePS'=6;
    [plAbovePONR] statePS=6 -> statePS'=6;
    [plBelowPONR] statePS=6 -> statePS'=6;
endmodule

module Button
    stateB : [0..6] init 0;       // pushed(1), released(3)
    [pushButton]    stateB=0 -> stateB'=1;
    [buttonP]       stateB=1 -> stateB'=2;
    [releaseButton] stateB=2 -> stateB'=3;
    [buttonR]       stateB=3 -> stateB'=0;
    [buFailsHigh] !(stateB=4 | stateB=5 | stateB=6)
        -> SensorFail: stateB'=4;
    [buttonP]      stateB=4 -> stateB'=6;
    [buFailsLow]  !(stateB=4 | stateB=5 | stateB=6)
        -> SensorFail: stateB'=5;
    [buttonR]       stateB=5 -> stateB'=6;
```

```
    [pushButton]     stateB=6 -> stateB'=6;
    [releaseButton]  stateB=6 -> stateB'=6;
endmodule

module Motor
    stateM : [0..3] init 0;       // on(1), off(3)
    [turnMOn]  stateM=0 -> stateM'=1;
    [motorOn]  stateM=1 -> stateM'=2;
    [turnMOff] stateM=2 -> stateM'=3;
    [motorOff] stateM=3 -> stateM'=0;
endmodule
```